MODULE V

Chapter 16. Comprehensive Case Study I: Cumene Process

16.1. Process Description

. Figure 16.1 provides a schematic of the cumene process along with the design and base-case salient operating conditions. Fresh benzene (C_6) and fresh propylene (0.95 propylene and 0.05 propane), mixed with recycle benzene are vaporized in a vaporizer. The vapor stream is preheated using the hot reactor effluent in a feed effluent heat exchanger (FEHE) before being heated to the reaction temperature in a furnace. The heated stream is fed into a packed bed reactor (PBR), a shell and tube heat exchanger with catalyst loaded tubes and pressurized coolant on the shell side. Propylene (C_3) and C_6 react in the vapor phase to produce cumene (C_9), which can further react with C_3 to produce a small amount of di-isopropyl benzene (C_{12} or DIPB) side product. The reactor effluent loses sensible heat in the FEHE and is partially condensed in a cooler. The cooled stream with C_9, C_{12}, unreacted reactants and inert propane is fed to a three column light-out-first distillation train. The purge column recovers inert propane and any unreacted propylene with some benzene as vapor distillate. The bottoms is sent to the recycle column which recovers the unreacted benzene as the distillate and recycles it. The recycle column bottoms is sent to the product column, which recovers nearly pure C_9 distillate and heavy C_{12} (+ some C_9) bottoms

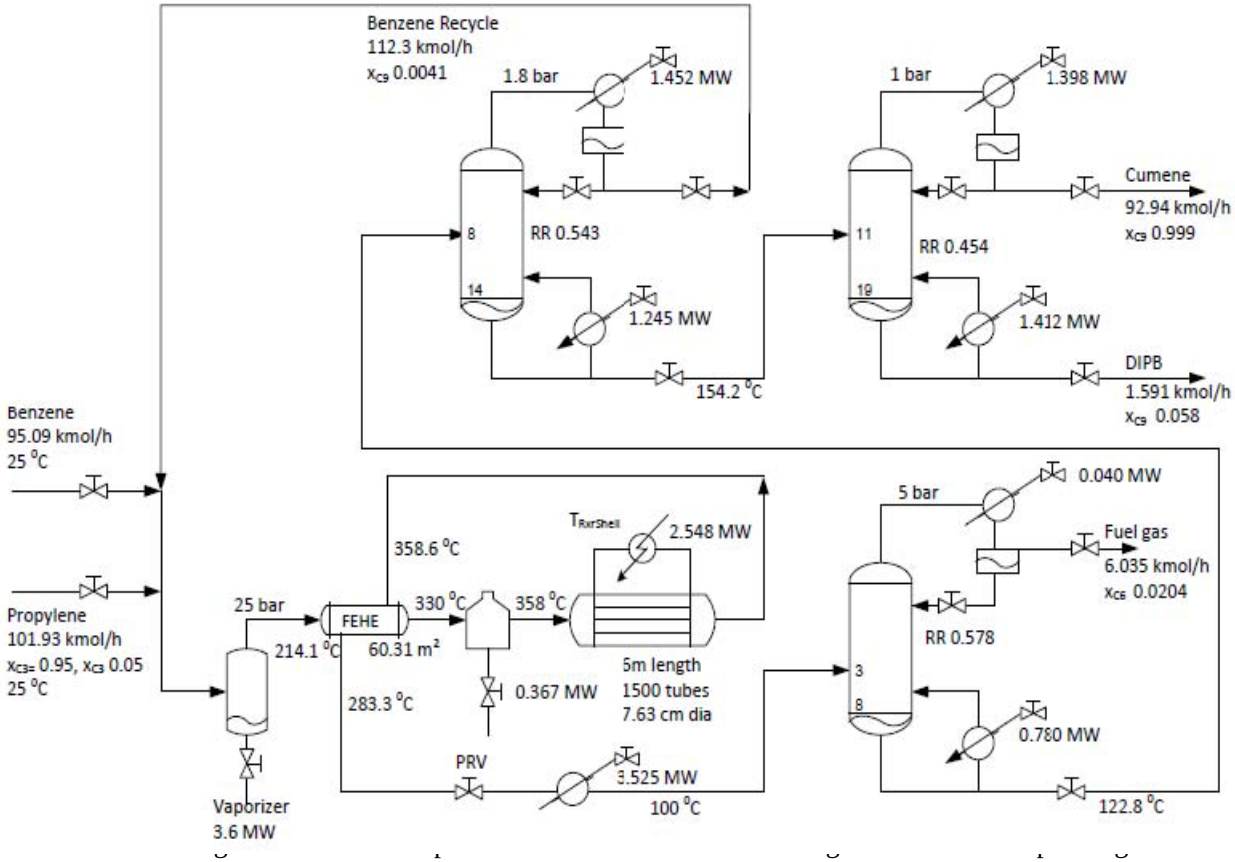

The reaction chemistry and kinetics used to model the process are provided in Table 16.1. The NRTL physical property method is used to model thermodynamic properties. Steady state simulation was performed using UniSim Design R390 version 3.61.0.0 from Honeywell. Luyben [19] has studied the design and basic regulatory control of a very similar cumene process flowsheet with the same reaction kinetics. The flowsheet studied here differs in that the first distillation column replaces a flash tank to mitigate loss of precious benzene in the C_3 fuel gas stream. The optimized base-case process design and steady state operating conditions are also shown in Figure 16.1. This revised design gives 6.8% higher profit [6] than Luyben's flowsheet.

Table 16.1. Reaction chemistry and kinetics

i	Reaction	k_i	$E_{a\,i}$ (kJ/kmol)	Concentration terms $f_i(C_j)$
1	$C6H6 + C_3H_6 - C_9H_{12}$	2.8 x 10^7	104174	$C_{C3}C_{C6}$
2	$C_9H_{12} + C_3H_6 - C_{12}H_{18}$	2.32 x 109	146742	$C_{C3}C_{C9}$
Objective	Maximize(J) J: hourly operating profit *			

Reaction rate $r_i = k_i.exp(-E_a^i/RT).f_i(C_j)$

C_j in kmol.m; r_i in kmol.m.s^{-3}.$^{-3}$.$^{-1}$

16.2. Economic Plantwide Control System (CS1) Design

16.2.1. Step 0: Optimal Steady State Process Operation

The plant has a total of 12 steady state operating degrees of freedom (DOFs): 1 each for the two fresh feeds, 1 for the furnace, 1 for reactor cooling, 1 for reactor pressure, 1 for reactor effluent cooler and 2 each for the three distillation columns. Specification variables corresponding to these degrees of freedom chosen for robust flowsheet convergence are: fresh propylene feed (F_{C3}), total benzene flow (F_{C6}^{Total}), reactor inlet temperature (T_{rxr}), reactor coolant temperature ($T_{RxrShell}$), reactor pressure (P_{Rxr}), reactor effluent cooler outlet temperature (T_{cooler}), $_{D1\ B1}$ first column vent temperature and bottoms propane mole fraction (T_{vent} and x_{C3}), the recycle $_{D2\ B2}$ column distillate cumene and the bottoms benzene mole fractions (x_{C9} and x_{C6}) and finally, $_{D3\ B3}$ the product column distillate cumene and the bottoms cumene mole fractions (x_{C9} and x_{C9}). These 12 specification variables can be adjusted to achieve a given objective such as maximum throughput/profit or maximum yield/selectivity.

In this work, the steady state hourly operating profit, P, defined as

P = *[Product Revenue – Raw Material Cost – Energy Cost] per hour* is used as a quantitative economic criterion that is maximized using the available steady state DOFs. We consider two modes of steady process operation. In Mode I, the desired throughput (production rate or feed processing rate) is specified, usually based on business considerations. For processes with undesirable side products, such as the cumene process considered here, the optimization typically attempts to maximize the yield to desired product. For processes with no undesirable side products (e.g. a separation train), the optimization attempts to minimize the energy consumption per kg product. In Mode II, the throughput itself is a decision variable for maximizing the economic criterion. Often, the Mode II solution corresponds to steady process operation at/near the maximum achievable throughput.

For the cumene process considered here, in Mode I, since the fresh propylene feed (F_{C3}) is fixed, only the remaining 11 DOFs need to be optimized. In Mode II, all 12 DOFs (including

F_{C3}) need to be optimized. The optimization is subject to physical and operational process constraints such as maximum / minimum material / energy flows, temperatures, pressures, product impurities etc.

Ideally all decision variables should be optimized simultaneously but this can result in an unwieldy problem with poor convergence. The optimization is therefore simplified by applying engineering reasoning to optimize only the dominant decision variables affecting the economic criterion with reasonable values for the remaining decision variables. For the cumene process, the reactor effluent cooler temperature (T_{cooler}) has very little impact on the economic objective function (P) and is therefore kept fixed at 100 °C, a reasonable value that ensures the reactor effluent vapor is condensed. Similarly, the yearly operating profit is insensitive to changes around the base design values of the propane mol fraction leaking down the first column bottoms (x_{C3}^{B1}) and the cumene mole fraction leaking up the second column distillate (x_{C9}^{D2}). These are therefore kept fixed at the base values. Also, the first column vapor vent stream temperature (T_{vent}^{D1}) is set by the cooling water at 32 °C.

These simple engineering arguments fix 4 specifications simplifying the optimization to 7 decision variables for Mode I (given F_{C3}) and 8 for Mode II. The optimization is performed using Matlab's *fmincon* routine with Unisim as the back-ground steady state flowsheet solver. The constrained optimization problem formulation (including price data and process constraints) and results for Mode I and Mode II are briefly summarized in Table 16.2.

The optimization results are interpreted as follows. The minimum product purity constraint ($x_{C9}^{D3,MIN}$ = 99.9%) is active in both Mode I and Mode II, i.e. at all throughputs, for on-aim product quality with no product give-away. The maximum reactor operating pressure (P_{Rxr}^{MAX}) and maximum recycle (second) column boilup (V_2^{MAX}) constraints are active at all throughputs. Reactor operation at maximum operating pressure causes the reactor temperature to be lower for a given conversion improving selectivity (cumene product yield). Recycle column operation at maximum boilup causes the total (fresh + recycle) benzene to the reactor to be as high as possible, again enhancing selectivity with a higher reactor benzene to propylene ratio. As throughput is increased, the product column maximum boilup constraint, V_3^{MAX}, goes active. Even as the throughput may be further increased by e.g. reducing the recycle column reflux (i.e. x_{C9}^{D2} is increased) and adjusting T_{Rxr} and $T_{RxrShell}$ to maintain conversion and selectivity, the Q_{fur}^{MIN} constraint goes active after which the selectivity decreases dramatically. The increase in throughput achieved is very marginal at < 1 kmol/h. We therefore treat V_3^{MAX} going active as corresponding to the maximum economic throughput (Mode II) with F_{C3} = 169.96 kmol/h.

The three Mode I active constraints ($x_{C9}^{D3,MIN}$, P_{Rxr}^{MAX} and V_2^{MAX}) along with the throughput specification (F_{C3}) leave four unconstrained DOFs. In Mode II, the throughput is not specified and gets determined by the value of the additional V_3^{MAX} constraint so that the number of unconstrained DOFs remains four. The unconstrained optimum values of the four decision variables, x_{C9}^{B3}, x_{C6}^{B2}, T_{Rxr} and $T_{RxrShell}$ are reported in Table 16.2 for Mode I and Mode II.

The low Mode I optimum x_{C9}^{B3} reduces the loss of precious cumene down the product column bottoms without a prohibitively high energy cost. The optimum Mode II x_{C9}^{B3} is much higher at 10%. This reduces the recycle column stripping load so that the V_3^{MAX} constraint goes active at higher throughputs for increased profit. Further loosening x_{C9}^{B3} however causes the profit to decrease due to excessive cumene loss in the side product stream.

The Mode I optimum benzene leakage down the recycle column bottoms, x_{C6}^{B2}, is on the higher side at 0.09% so that benzene is the principal cumene product impurity. This is reasonable as benzene is the cheaper product impurity with DIPB consuming 2 extra mols of propylene. The

Mode II optimum x_{C6}^{B2} value reduces to 0.05% so that the two product impurities are comparable. As shown in Figure 16.2, this balances throughput and selectivity with V_2^{MAX} and V_3^{MAX} active constraints. If x_{C6}^{B2} is too high, the DIPB leakage in the product column distillate is prohibitively small requiring high reflux so that the V_3^{MAX} constraint goes active at a significantly lower throughput. Similarly, if x_{C6}^{B2} is too low, the feed that can be processed by the recycle column maintaining its two separation specifications without violating the V_2^{MAX} constraint is lower implying a loss in throughput. Also, as x_{C6}^{B2} is loosened, with V_2^{MAX} active, the benzene recycle increases for better selectivity with lower DIPB formation. Comparable amounts of the two principal impurities in the product balances these two effects.

Table 16.2. Process optimization formulation and results' summary

i	Reaction	k_i	$E_{a\,i}$ (kJ/kmol)	Concentration terms $f_i(C_j)$
1	$C_6H_6 + C_3H_6 - C_9H_{12}$	2.8 x 10^7	104174	$C_{C3}C_{C6}$
2	$C_9H_{12} + C_3H_6 - C_{12}H_{18}$	2.32 x 109	146742	$C_{C3}C_{C9}$

Objective	Maximize(J) J: hourly operating profit *	
Process Constraints	*0 ≤ Material Flows ≤ 2 (base case) 0 ≤ V_1, V_2, V_3 ≤ 1.5 (base case) Vent Temperature = 32 ^oC 0 ≤ Energy Flows ≤ 1.7 (base case) 1 bar ≤ P_{Rxr} ≤ 25 bar Cumene Product Purity ≥ 0.999 mol fraction*	
Decision Variable	Mode I	Mode II
$FC3$	101.93 kmol/h Fixed	169.96 kmol/h
$F_{C6\ Total}$	294.16 kmol/h	316.2 kmol/h
$Trxr$	322.26 °C	318.58 °C
$TRxrShell$	368.95 °C	367.98 °C
$PRxr$	25 bar Max	25 bar Max
$Tcooler$	100 °C Fixed	100 °C Fixed
$T_{vent\ D1}$	32 °C Fixed	32 °C Fixed
$x_{C3\ B1}$	0.1 % Fixed	0.1 % Fixed
$x_{C9\ D2}$	0.4 % Fixed	0.4 % Fixed
$x_{C6\ B2}$	0.09 %	0.05 %
$x_{C9\ D3}$	99.9 % Min	99.9 % Min
$x_{C9\ B3}$	0.4 %	10 %
Optimum J F_{C9} Active Constraints	\$3.809x10^3 h^{-1} 93.59 kmol/h $x_{C9\ D3\ MIN}$, $P_{Rxr\ MAX}$, $V_{2\ MAX}$	\$5.879x10^3 h^{-1} 150.045 kmol/h $x_{C9\ D3\ MIN}$, $P_{Rxr\ MAX}$, $V_{2\ MAX}$, $V_{3\ MAX}$

SNo	CV	Remarks on regulatory / economic significance
1	F_{C3}	Determines process throughput. Maximum throughput limited by $V_{3\ MAX}$
2	$F_{C6\ Total}$	Increasing F_{C6Tot} improves selectivity. Maximum F_{C6Tot} limited by $V_{2\ MAX}$. Affects reactor conversion and selectivity.
3	T_{rxr}	Stabilizes reaction heat recycle through FEHE. Affects reactor conversion and selectivity.
4	$T_{RxrShell}$	Stabilizes reaction heat removal. Operate at $P_{Rxr\ MAX}$ for maximum reactor conversion.
5	P_{Rxr}	Stabilizes gas inventory in reaction section.

*: Heater duty \$16.8 GJ^{-1}; Steam \$9.83 GJ^{-1};Cooling water \$0.16 GJ^{-1};F_{C6} \$ 68.5$kmol^{-1}$; F_{C3} \$ 34.3$kmol^{-1}$; F_{C9} \$ 150.0$kmol^{-1}$

We now seek a simple steady state operating policy that ensures near optimal operation over the entire throughput range. For economically optimal operation, we would like tight control of the active constraints and appropriate management of the remaining unconstrained steady state DOFs using SOVs. Preferably, the CVs corresponding to the unconstrained steady state DOFs should be measurements that are cheap, reliable, fast, robust and dynamically well

behaved with respect to the manipulated variables (MVs). These CVs should therefore be flow, pressure and temperature based avoiding cumbersome analytical measurements.

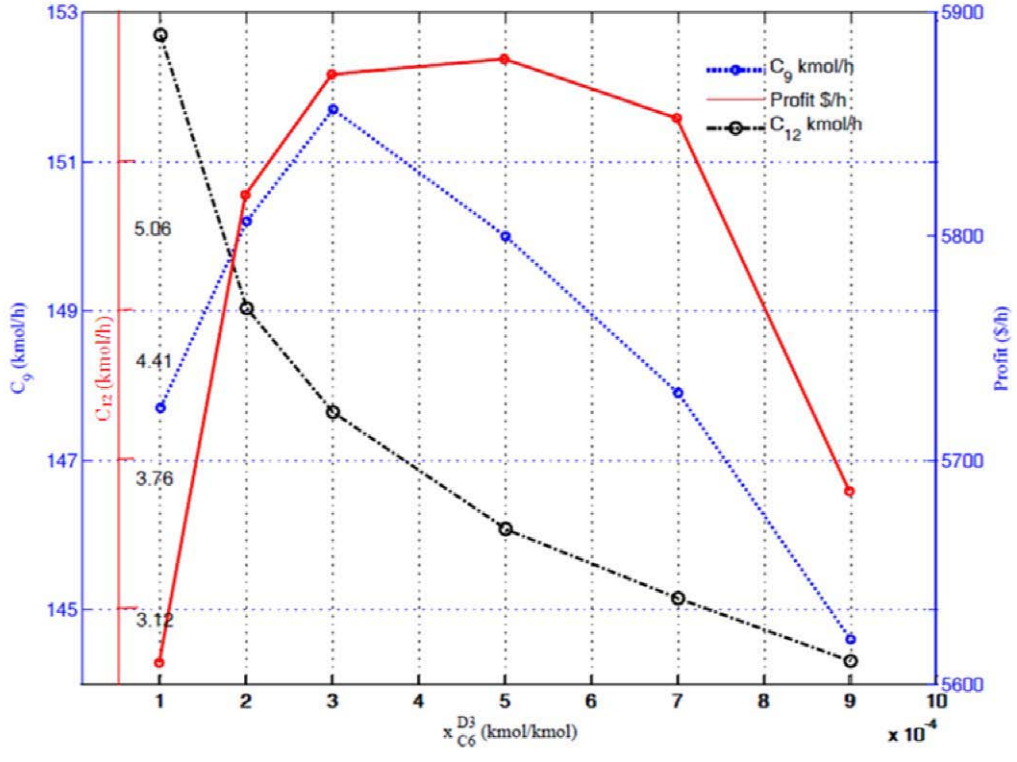

Figure 16.2. Optimum benzene impurity level in cumene product

Of the 12 decision variables in Table 16.2, 4 decision variables, T_{vent}, T_{Cooler}, x_{C3}^{B1} and $x_{C9}^{D2\ D3\ MIN}$ were fixed at reasonable values. In Mode I, there are three active constraints, $x_{C9}^{MAX\ MAX\ MAX}$, P_{Rxr} and V_2 along with a specified F_{C3}. In Mode II, V_3 going active sets F_{C3}. Optimum values for the remaining 4 unconstrained decision variables in both modes, T_{Rxr}, $T_{RxrShell}$, x_{C6}^{D3} and x_{C9}^{B3} were obtained.

In the above set of variables, compositions not related to the product quality, i.e., x_{C3}^{B1}, $x_{C9}^{D2\ B3}$ and x_{C9} would usually not be available. Accordingly, we consider using appropriate temperature inferential measurements. On the purge and product columns, controlling appropriate sensitive stripping tray temperatures, T_{Col1}^{S} and T_{Col3}^{S}, respectively, would regulate the light key leakage down the bottoms. This would indirectly maintain x_{C3}^{B1} and x_{C9}^{B3} within a small band. On the recycle column, maintaining the reflux (L_2) in ratio with the column feed (B_1) would regulate the distillate cumene leakage (x_{C9}^{D2}). The product DIPB impurity mol fraction (x_{C12}^{D3}) and benzene impurity mol fraction (x_{C6}^{D3}) measurements would usually be available in an industrial setting. For on-aim product cumene mol fraction ($x_{C9} = x_{C9}^{D3\ D3MIN\ D3} = 99.9\%$), $x_{C6}^{D3\ D3}$ + $x_{C12} = 0.1\%$ so that only one of the impurity mol fractions is independent. We take x_{C6} to be independent with $x_{C12} = 0.1\% - x_{C6}$.

The revised practical CVs corresponding to the 12 steady state DOFs are tabulated in Table 16.3 along with their regulatory and economic significance. The CVs are the active constraints (or specifications) and four unconstrained CVs, T_{Rxr}, $T_{RxrShell}$, x_{C6}^{D3} and T_{Col3}^{S}. Of the unconstrained CVs, the optimum reactor inlet temperature (T_{Rxr}) and reactor coolant temperature

($T_{RxrShell}$) are nearly the same for Mode I and Mode II (see Table 16.2). Holding these two variables constant would likely be near optimal across the wide throughput range. For the remaining two CVs, since economic losses per unit deviation away from the optimum values are usually the highest at maximum throughput, we consider implementing the Mode II optimum value at the lower throughputs. This gives a very simple constant setpoint policy across the entire throughput range. To quantify the economic loss entailed, Figure 16.3 compares the variation with throughput in the optimum operating profit and the operating profit using the constant Mode II setpoints for the above four CVs. The constant setpoint operating policy provides near optimal steady operation with the maximum profit loss being < 0.21%. These four CVs may thus be deemed as SOVs that provide near optimum steady operation across the entire throughput range.

Table 16.3. Revised practical CVs

i	Reaction	k_i	$E_{a\,i}$ (kJ/kmol)	Concentration terms $f_i(C_j)$
1	$C6H6 + C_3H_6 - C_9H_{12}$	2.8 x 10^7	104174	$C_{C3}C_{C6}$
2	$C_9H_{12} + C_3H_6 - C_{12}H_{18}$	2.32 x 109	146742	$C_{C3}C_{C9}$

Objective	Maximize(J) J: hourly operating profit *	
Process Constraints	*0 ≤ Material Flows ≤ 2 (base case) 0 ≤ V_1, V_2, V_3 ≤ 1.5 (base case) Vent Temperature = 32 ^oC 0 ≤ Energy Flows ≤ 1.7 (base case) 1 bar ≤ P_{Rxr} ≤ 25 bar Cumene Product Purity ≥ 0.999 mol fraction*	
Decision Variable	Mode I	Mode II
$FC3$	101.93 kmol/h Fixed	169.96 kmol/h
$F_{C6\ Total}$	294.16 kmol/h	316.2 kmol/h
$Trxr$	322.26 °C	318.58 °C
$TRxrShell$	368.95 °C	367.98 °C
$PRxr$	25 bar Max	25 bar Max
$Tcooler$	100 °C Fixed	100 °C Fixed
$T_{vent\ D1}$	32 °C Fixed	32 °C Fixed
$x_{C3\ B1}$	0.1 % Fixed	0.1 % Fixed
$x_{C9\ D2}$	0.4 % Fixed	0.4 % Fixed
$x_{C6\ B2}$	0.09 %	0.05 %
$x_{C9\ D3}$	99.9 % Min	99.9 % Min
$x_{C9\ B3}$	0.4 %	10 %
Optimum J F_{C9} Active Constraints	\$3.809x10^3 h $^{-1}$ 93.59 kmol/h $x_{C9\ D3\ MIN}$, $P_{Rxr\ MAX}$, $V_{2\ MAX}$	\$5.879x10^3 h $^{-1}$ 150.045 kmol/h $x_{C9\ D3\ MIN}$, $P_{Rxr\ MAX}$, $V_{2\ MAX}$, $V_{3\ MAX}$

SNo	CV	Remarks on regulatory / economic significance
1	F_{C3}	Determines process throughput. Maximum throughput limited by $V_{3\ MAX}$
2	$F_{C6\ Total}$	Increasing F_{C6Tot} improves selectivity. Maximum F_{C6Tot} limited by $V_{2\ MAX}$. Affects reactor conversion and selectivity.
3	T_{rxr}	Stabilizes reaction heat recycle through FEHE. Affects reactor conversion and selectivity.
4	$T_{RxrShell}$	Stabilizes reaction heat removal. Operate at $P_{Rxr\ MAX}$ for maximum reactor conversion.
5	P_{Rxr}	Stabilizes gas inventory in reaction section.
6	$x_{C6\ D3}$	Determines benzene impurity level in product. Fixed by benzene dropping down the recycle column.

16.2.2. Step 1: Loops for Tight Economic CV Control

The hard active constraints at maximum throughput are V_2 and V_3. These are economically important as a back-off from $V_{2\ MAX}$ reduces the benzene recycle rate with loss in reactor selectivity while a back-off in $V_{3\ MAX}$ causes a loss in throughput. To minimize the back-off, V_2 and V_3 are controlled tightly using the respective reboiler duties (Q_{Reb2} and Q_{Reb3}).

P_{Rxr}^{MAX}, another economically important active constraint due to its impact on the reactor conversion, is considered a soft constraint. The reactor pressure is controlled tightly around its maximum value ($P_{Rxr} = P_{Rxr}^{SP,MAX}$) by manipulating the pressure regulatory valve (PRV) between the reaction and separation sections. The pairing would provide tight control.

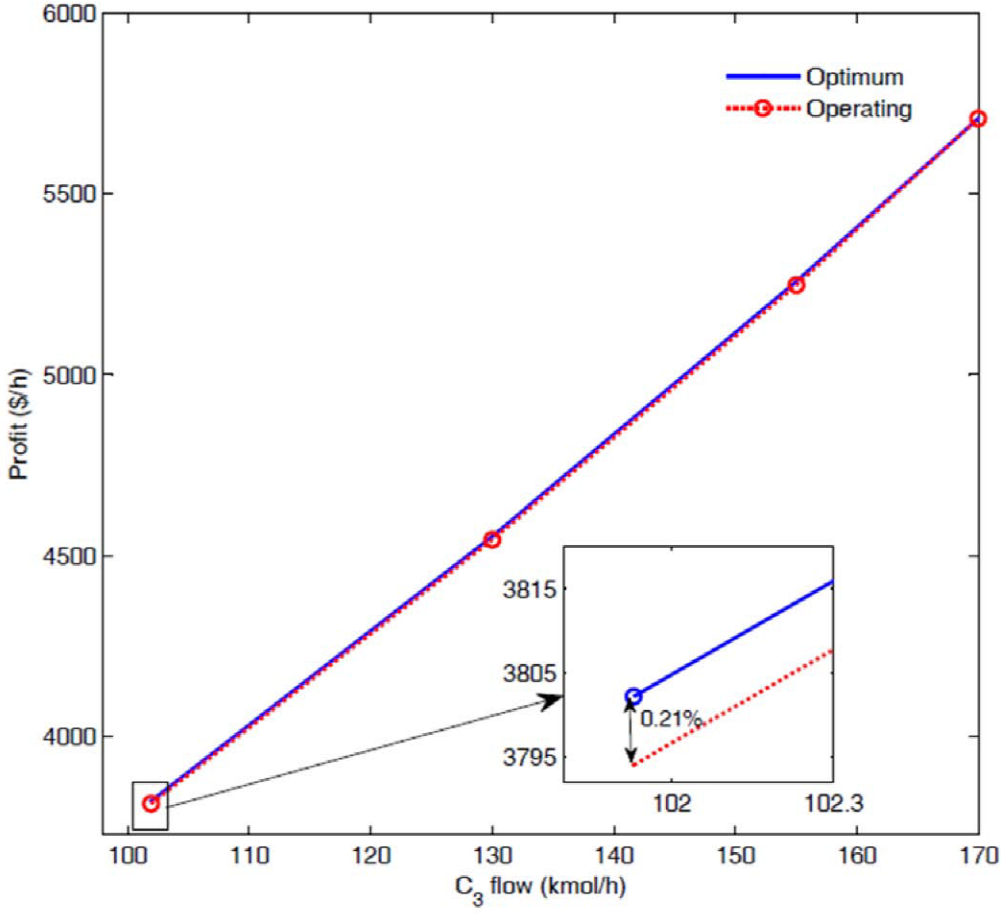

Figure 16.3. Comparison of optimum steady profit and achieved profit using simple constant setpoint operating policy at various throughputs

Economic operation requires tight control of the product impurity levels for on aim product purity of x_{C9}, a soft active constraint. For maintaining $x_{C9}^{D3,MIN D3}$, the two principal impurities in the product, C_{12} and C_6, must be maintained. Control of x_{C12}^{D3} is accomplished by adjusting the product column reflux to feed ratio (L_3/B_2). The ratio scheme helps mitigate the variability in x_{C12}^{D3} due to the feedforward action of the ratio controller to column feed flow disturbances. With regard to the C_6 impurity in the product, note that all the benzene that leaks down the recycle column ends up in the product. Tight regulation of the benzene leakage down the recycle column can be achieved by maintaining a stripping tray temperature (T_{Col2}^{S}). Since V_2^{MAX} constraint is active, we may use the feed to the recycle column (B_1) or the recycle column reflux rate (L_2) as the MV. The former would be effective for a mostly liquid feed and the latter must be used for a mostly vapor feed. For the specific choice of the design pressures of the purge and recycle columns, the B_1 vapor fraction is ~25% so that the T_{Col2}^{S} -B_1 pairing is selected. The

$T_{Col2}^{S,SP,D3}$ is adjusted by a x_{C6} composition controller. The product impurity mol fraction

setpoints are chosen as x_{C6}^{D3SP} = 0.05% (Mode II optimum value) and x_{C12}^{D3SP} = 0.1% - x_{C6}^{D3SP} = 0.05%. These setpoints are held constant at lower throughputs for near optimal operation. Economic operation requires the cumene leakage down the product column bottoms to be small. This is achieved by maintaining a product column stripping tray temperature (T_{Col3}^{S}). MAX_S

Since V_3 is active and the column feed (B_2) is mostly liquid, the T_{Col3} -B_2 pairing is chosen.

Lastly, maintaining a high reactor conversion for a small propylene loss in the fuel gas stream as well as a high reactor selectivity for small loss of precious raw materials as DIPB by-product are economically important objectives. Holding the reactor inlet temperature constant at 322 °C and the reactor shell side coolant temperature at 367 °C ensure that the reactor conversion and selectivity are maintained at high values across the entire throughput range. T_{Rxr} is controlled tightly by manipulating the furnace duty (Q_{fur}) for tight control. $T_{RxrShell}$ = 367 °C is a direct input (MV) to the process as the constant coolant temperature model is used in the simulations. In practice, since the reactor temperature is high, a proprietary heating oil such as Dowtherm would be used as the coolant with high pressure steam being generated in a downstream Dowtherm heated boiler. $T_{RxrShell}$ then is controlled by adjusting the boiler pressure setpoint with the boiler pressure being controlled by the exit steam flow.

16.2.3. Step 2: Inventory Control System Design

We now pair loops for inventory regulation, inventory being interpreted in its most comprehensive sense to include total material, phase, components and energy. Of the 12 steady state DOFs, 8 loops have already been implemented in Step 1. This leaves 4 additional loops that need to be configured plus loops for regulating the reflux drum and bottom sump levels on the three columns along with the column pressures and the feed vaporizer level.

The 4 additional loops correspond to holding L_2/B_1, T_{vent}, T_{Col1}^{S} and T_{Cooler} at their design values. Maintaining L_2/B_1 using a feed to reflux ratio controller regulates the C_9 leakage in the benzene recycle stream. The purge column condenser temperature is controlled by manipulating its condenser duty (Q_{Cnd1}). This regulates the loss of precious benzene in the fuel gas stream. The purge column stripping tray temperature (T_{Col1}^{S}) is controlled using its boilup (V_1) to regulate the C_3 leakage down the bottoms. The reactor effluent condensate temperature (T_{Cooler}) is controlled by manipulating the effluent cooler duty (Q_{Cooler}). This ensures proper regulation of the gas/vapor inventory in the reaction section in conjunction with the P_{Rxr} control loop.

The recycle and product column pressures (P_{Cnd1} and P_{Cnd2}) are regulated by the respective condenser duty valves, Q_{Cnd2} and Q_{Cnd2}. The purge column pressure (P_{Col1}) is regulated by the vent rate, D_1. Its reflux drum level (LVL_{RD1}) is regulated by manipulating the reflux (L_1). The feed vaporizer level (LVL_{Vap}) is regulated by the vaporizer duty (Q_{Vap}). The recycle column and product column reflux drum levels (LVL_{RD2} and LVL_{RD3}) are regulated using the respective distillate rates (D_2 and D_3). The product column bottom sump level (LVL_{Bot3}) is regulated using its bottoms rate (B_3). With these pairings, no close-by valves are left for regulating the purge column and recycle column bottom sump levels (LVL_{Bot1} and LVL_{Bot2}). The only option is to manipulate the two fresh feeds, F_{C3} and F_{C6}. C_3 is the limiting reactant with near complete single-pass conversion so that F_{C3} determines the cumene and DIPB production in the reactor. Since the cumene and DIPB accumulate at the bottom of the recycle column, the LVL_{Bot2} -F_{C3} pairing is implemented for recycle column sump level control with the LVL_{Bot1} -F_{C6} pairing being implemented for purge column sump level control.

16.2.4. Step 3: Throughput Manipulation and Additional Economic Loops

In this example, there is only one active constraint region corresponding to V_3^{MAX} going active at maximum throughput with the other constraints / specifications being fixed at their Mode II values at lower throughputs. The throughput may be reduced by reducing V_3 below V_3^{MAX}. V_3^{SP} is then the throughput manipulator (TPM) adjusted to operate the plant at the desired throughput below maximum. There are no additional SOVs whose control needs to be taken up at lower throughputs as no additional constraints become inactive at lower throughputs.

The economic plantwide control structure, labeled CS1, obtained by the application of Step 1-3 is shown in Figure 16.4 with the economic loops in blue. CS1 has been designed for the tightest possible control of the economic CVs using close by MVs. Since control valves get used up in these loops, in the inventory control system, the MVs of the bottom sump level loops for the purge and recycle columns are not local to the respective units but away at the fresh feeds and thus very unconventional. Even so, acceptable level regulation is expected as the lag associated with the reaction section is small with the material essentially flowing through a long pipe with small vaporizer and the reactor effluent cooler lags. The acceptable level regulation and overall process stabilization was confirmed from rigorous dynamic simulations. With the unconventional long level loops, the control structure attempts tight control of the economic CVs with loose level control. In other words, the structure attempts tight control of the economic CVs by transforming the transients to the surge levels that have no steady state economic impact.

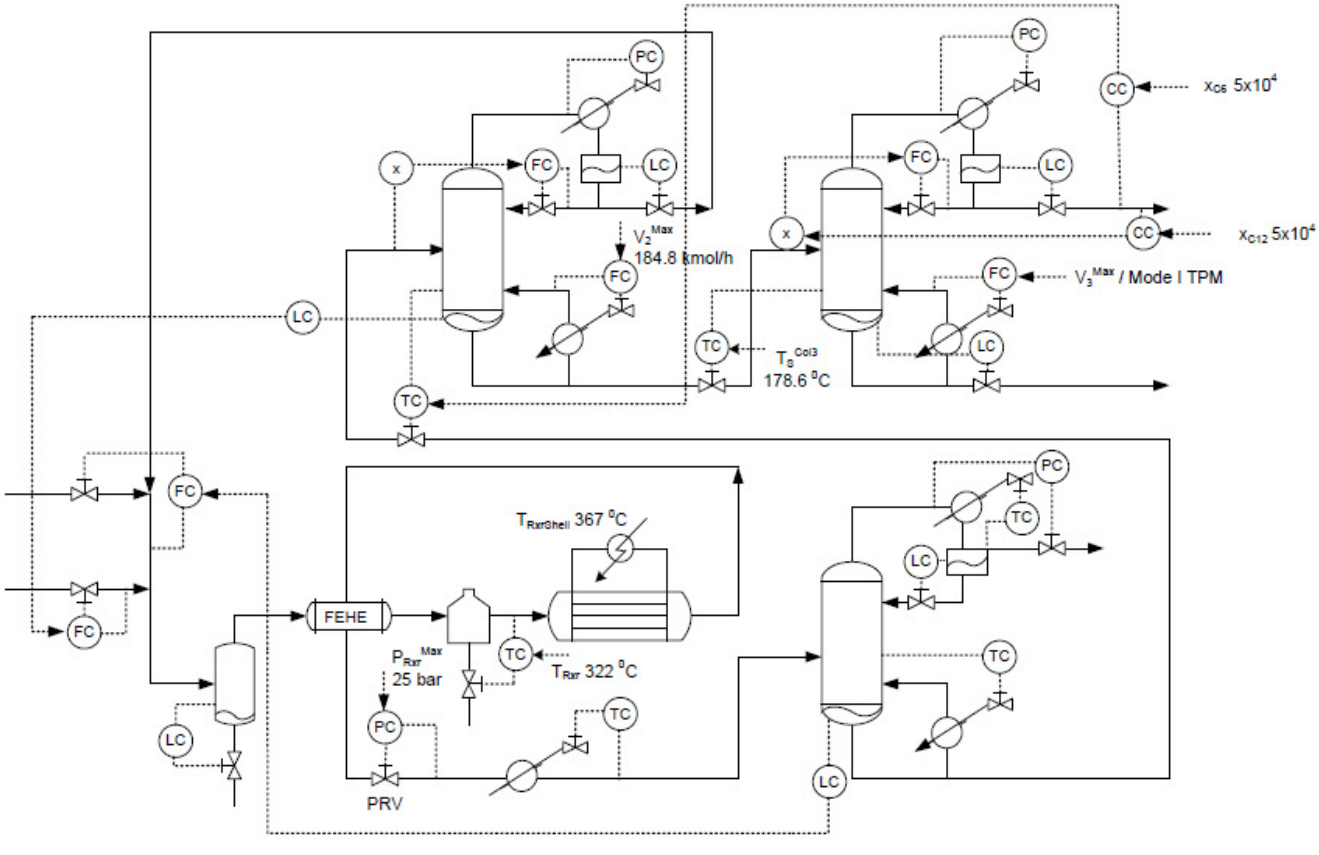

16.3. Conventional Plantwide Control Structure (CS2)

The conventional plantwide control structure, CS2, with the TPM at the C_3 (limiting reactant) feed is shown in Figure 16.5. The total benzene (fresh + recycle) is maintained by F_{C6Tot} to prevent snowballing in the benzene recycle loop. In the reaction section, LVL_{Vap} is controlled by Q_{Vap}, T_{Rxr} is controlled by Q_{Fur}, $T_{RxrShell}$ is set at its near optimum value, P_{Rxr} is controlled at P_{Rxr}^{MAX} by the PRV and the partially condensed reactant effluent temperature (T_{Cooler}) is maintained by its cooling duty, Q_{Cooler}. In the separation train, the recycle and product column pressures are controlled by the respective condenser duties, the reflux drum levels using the respective distillate streams and the bottom sump levels using the respective bottoms streams. On the purge column, the column pressure is controlled by the vapor vent, the overhead condenser temperature is maintained by the condenser duty and the reflux drum level is controlled by the reflux. To regulate the C_3 leakage down the bottoms, T_{Col1}^{S} is maintained by V_1. On the recycle column, L_2 is maintained in ratio with the column feed (B_1) and T_{Col2}^{S} is maintained by V_2 with

$T_{Col2}^{S\,SP\,D3}$ being adjusted to maintain the product impurity x_{C6}. On the product column, the reflux (L_3) is maintained in ratio with the feed (B_2) and L_3/B_2^{SP} is adjusted to maintain the product impurity x_{C12}^{D3}. T_{Col3}^{S} is maintained by adjusting V_3.

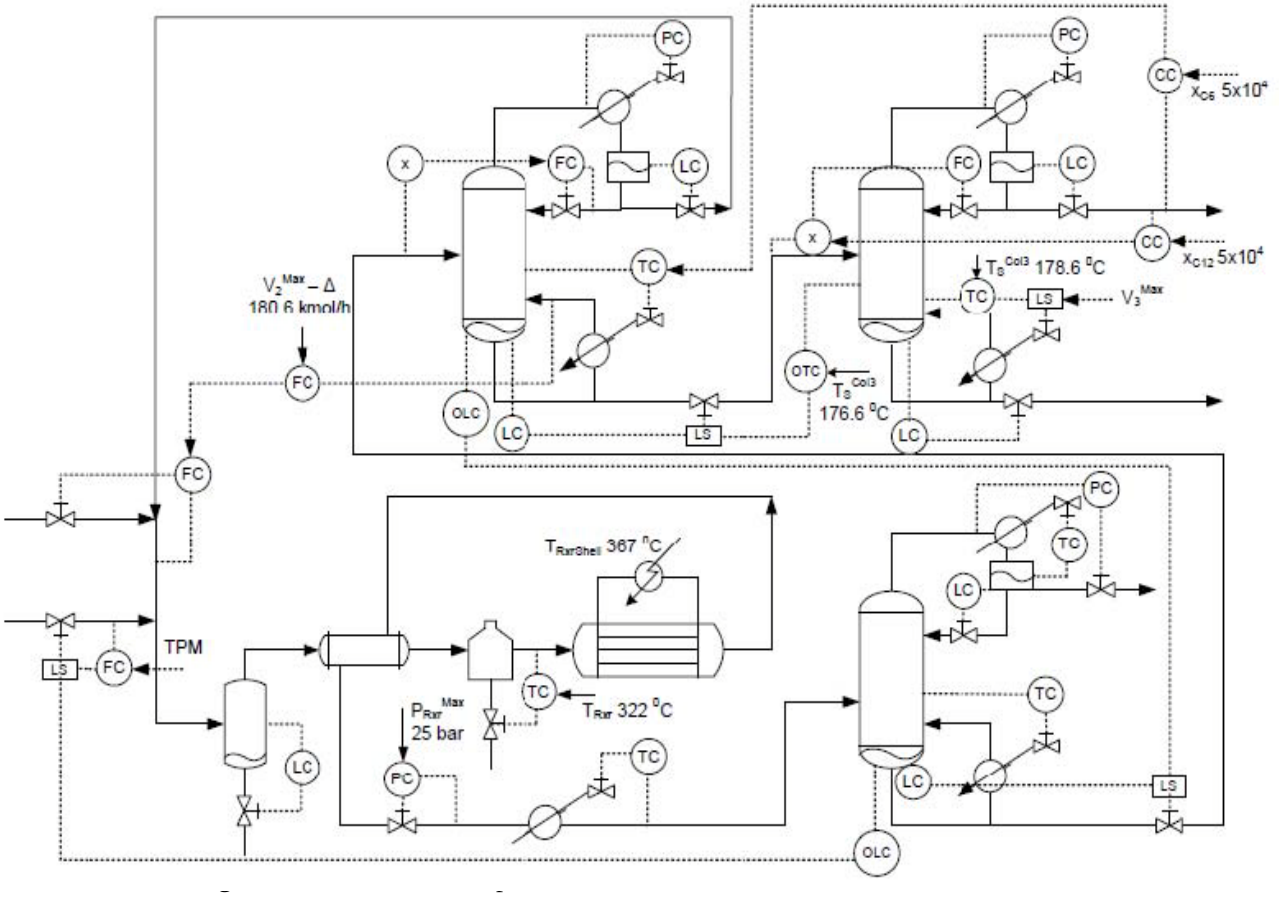

Since optimal operation requires running the process at V_2^{MAX} at all throughputs, a supervisory controller is installed that adjusts the total benzene setpoint (F_{C6Tot}^{SP}) to maintain V_2

at its setpoint. Since V_2^{MAX} is a hard constraint corresponding to the initiation of recycle column flooding and since control of the stripping tray temperature (T^S_{Col2}) must never be lost to ensure the product benzene impurity level is always regulated, some back-off from the V_2^{MAX} limit would be needed to ensure the hard constraint is not violated during worst case transients.

The other hard constraint that must be handled is V_3^{MAX}, the bottleneck constraint, which goes active as throughput is increased towards maximum. When V_3^{MAX} goes active, product column temperature control (T^S_{Col3}) is lost implying loss of precious cumene down the bottoms with a severe economic penalty. To avoid the same, an override control system is put in place that alters the material balance control structure all the way up to the C_3 feed to ensure that column temperature control is not lost when V_3^{MAX} goes active, as in Figure 16.5.

The override scheme works as follows. The override temperature controller on the product column is direct acting and has its setpoint slightly below the T^S_{Col3}-V_3 loop setpoint. Thus when V_3^{MAX} is inactive, its output is high (usually saturated) and B_2 controls the recycle column sump level. When V_3^{MAX} goes active, product column temperature decreases below the second temperature controller setpoint and its output ultimately decreases below the LVL_{Bot2} controller output with the low select passing the manipulation of B_2 from the LVL_{Bot2} controller to the override temperature controller. Once this occurs, LVL_{Bot2} control is lost and it rises. The second LVL_{Bot2} override controller then takes over manipulation of B_1 via the low select in a manner similar to the product column temperature override scheme. This causes LVL_{Bot1} control to be lost and the second LVL_{Bot1} override controller ultimately takes over F_{C3} manipulation. The override scheme thus works to cut down on the fresh propylene feed on V_3^{MAX} going active.

16.4. Dynamic Simulation Results and Discussion

Rigorous dynamic simulations are performed in Unisim to evaluate and compare the performance of the synthesized economic plantwide control structure, CS1, with the conventional plantwide control structure, CS2.

16.4.1. Controller Tuning

A consistent procedure is used to tune the various controllers. All flow and pressure controllers are PI and tuned for a fast and snappy response. All conventional level controllers with local unit specific pairings are P only and use a gain of 2 to smooth out flow transients. The temperature controllers are PI with a 45 s sensor lag. The Unisim autotuner is used to obtain a reasonable value of the reset time and controller gain (K_C). The K_C is then adjusted for a fast but not-too-oscillatory servo response. All composition controllers use a sensor dead-time and sampling time of 5 mins. The autotuner does not provide reasonable initial tuning parameters so that the open loop response is first obtained and the reset time set to 2/3rd open loop response completion time and K_C set to the inverse of the process gain. These tunings work well for the two product impurity controllers in both CS1 and CS2.

In CS1, the unconventional non-local LVL_{Bot1} and LVL_{Bot2} controllers are P only and are tuned initially by hit and trial to stabilize the process. The temperature and composition loops are then tuned as discussed above. Finally, the non-local level controller tunings are further refined for a smooth overall plantwide response to the principal disturbances. In CS2, the product column override temperature controller setpoint is chosen to the highest possible value so that the over-ride controller never goes active for the different disturbance scenarios. This gives a

setpoint that is 2 °C below nominal. The LVL_{Bot1} and LVL_{Bot2} override setpoints are chosen 10% above the nominal setpoint of 50%. Also, aggressive tuning is attempted to ensure F_{C3} is cut quickly when V_3 goes active to mitigate the loss of precious cumene down the product column bottoms during the transient. Both the over ride level controllers are P only. Finally the supervisory recycle column boilup controller is tuned for a not-too-oscillatory servo response. The salient controller tuning parameters and setpoints thus obtained are reported in Table 16.4 for CS1 and CS2.

Table 16.4. CS1 and CS2 controller parameters[*#]

i	Reaction	k_i	$E_{a\,i}$ (kJ/kmol)	Concentration terms $f_i(C_j)$
1	$C6H6 + C_3H_6 - C_9H_{12}$	2.8 x 10^7	104174	$C_{C3}C_{C6}$
2	$C_9H_{12} + C_3H_6 - C_{12}H_{18}$	2.32 x 109	146742	$C_{C3}C_{C9}$

Objective	Maximize(J) J: hourly operating profit *	
Process Constraints	*0 ≤ Material Flows ≤ 2 (base case) 0 ≤ V_1, V_2, V_3 ≤ 1.5 (base case) Vent Temperature = 32 ^oC 0 ≤ Energy Flows ≤ 1.7 (base case) 1 bar ≤ P_{Rxr} ≤ 25 bar Cumene Product Purity ≥ 0.999 mol fraction*	
Decision Variable	Mode I	Mode II
$FC3$	101.93 kmol/h Fixed	169.96 kmol/h
$F_{C6\ Total}$	294.16 kmol/h	316.2 kmol/h
$Trxr$	322.26 °C	318.58 °C
$TRxrShell$	368.95 °C	367.98 °C
$PRxr$	25 bar Max	25 bar Max
$Tcooler$	100 °C Fixed	100 °C Fixed
$T_{vent\ D1}$	32 °C Fixed	32 °C Fixed
$x_{C3\ B1}$	0.1 % Fixed	0.1 % Fixed
$x_{C9\ D2}$	0.4 % Fixed	0.4 % Fixed
$x_{C6\ B2}$	0.09 %	0.05 %
	99.9 %	99.9 %

*: All level loops use K_C = 2 unless otherwise specified #: Pressure/flow controllers tuned for tight control

16.4.2. Closed Loop Results

CS1 and CS2 are dynamically tested for different disturbance scenarios. First, the dynamic transition from Mode I to Mode II is simulated. The dynamic response is also obtained for a ±10% throughput step change and a ±3% step change in the feed propylene mol fraction for Mode I (F_{C3} = 101.93 kmol/h) operation. For Mode II, the dynamic response is obtained for the latter as well as a ±5% step bias in the F_{C3} flow sensor. For convenience, the CS2, supervisory V_2 controller setpoint is set at V_2^{MAX} even as in practice sufficient back-off would be provided to ensure the hard V_2^{MAX} constraint is never violated during worst case transients and benzene impurity control in the product cumene is never lost.

We first consider throughput transition using CS1 and CS2, from Mode I (low throughput) to Mode II (maximum throughput) and back. In both structures, the TPM is ramped at a rate that causes F_{C3} to change by ~10 kmol in 15 hrs. This ensures that the severity of the throughput transition disturbance is comparable in both the structures. For the throughput

transition in CS1, V_3, is ramped up at a rate of 0.79 kmol/h to V_3^{SPMAX}, held constant for 20 hours and then ramped back down at the same rate. In CS2, F_{C3}^{SP} is ramped at a rate of 0.74 kmol/h till 184 kmol/h (or lower if override takes over F_{C3} manipulation), held there for about 30 hours to

allow for the over-rides to take over and stabilize and then ramped back down to 101.93 kmol/h. As recommended by Shinskey[21], we use external reset on the PI T^{S}_{Col3} override controller to ensure it takes up B_2 manipulation at the earliest once V_3^{MAX} goes active.

The CS1 and CS2 transient response of salient process variables is plotted in Figure 16.6. Tight product purity control as well as smooth plantwide transients are observed for both CS1 and CS2. In CS2, the major events of V_3^{MAX} going active (P_1), the ethylene feed being cut by the LVL_{Bot1} override (P_2) and beginning of the F_{C3}^{SP} (TPM) ramp down (P_3) are shown. In the CS2 dynamic response, oscillations post LVL_{Bot1} override controller taking over F_{C3} manipulation are seen. Also it takes about 5 hrs between V_3^{MAX} going active and F_{C3}^{SP} manipulation passing to the B_3^{MAX} LVL_{Bot1} override. The transient x_{C9} response for CS1 and CS2 also shows that once V_3 goes active, the cumene leakage in the DIPB stream remains well regulated in CS1 while in CS2 the leakage increases due to the lower T^{S}_{pur} override setpoint. In the entire transient period, LVL_{Bot1} and LVL_{Bot2} vary within a band of 15% and 24% respectively, in CS1. The corresponding figures for CS2 are comparable at 16% and 24% respectively.

To compare the structures for Mode II operation, Figure 16.7 plots the dynamic response of important process variables to a ±5% step bias in the F_{C3} measurement for CS1 and CS2. The dynamic response for CS1 achieves tight product purity control with a settling time of about 10 hours. Similarly, the CS2 transient response also completes in about 10 hours. Note that since V_3^{MAX} is active, the CS2 T_{Col3}, LVL_{Bot2} and LVL_{Bot1}^{S} overrides are on and the material balance control structure is oriented in the reverse direction of process flow.

To compare the structures for Mode I operation, Figure 16.8 plots the plantwide dynamic response of important process variables to a step change in the TPM for a ±10% throughput change. In CS1, to bring about a 10% increase and decrease in F_{C3}, the V_3^{SP} must be changed by +22.1 kmol/h and -21.9 kmol/h, respectively. In CS2, F_{C3} is directly set by F_{C3}^{SP} (TPM). The product purity and DIPB cumene loss control in CS2 is not as tight as in CS1 as the TPM for CS1 is located at the product column. In CS2, on the other hand, the TPM is at a process feed and the downstream product column gets subjected to a less severe transient due to filtering by the intermediate units. Overall, a smooth plantwide response is observed in both structures. The response completion time for CS1 and CS2 is slightly above and below 10 hrs, respectively.

Figure 16.9 compares the plantwide response of important process variables to a ±3% step change in the C_3 feed propane (inert) impurity in Mode I operation. Both structures handle the disturbance well with the product purity being tightly controlled. The overall plantwide response is also smooth with a response settling time of about 15 hrs for CS1 and about 10 hrs for CS2.

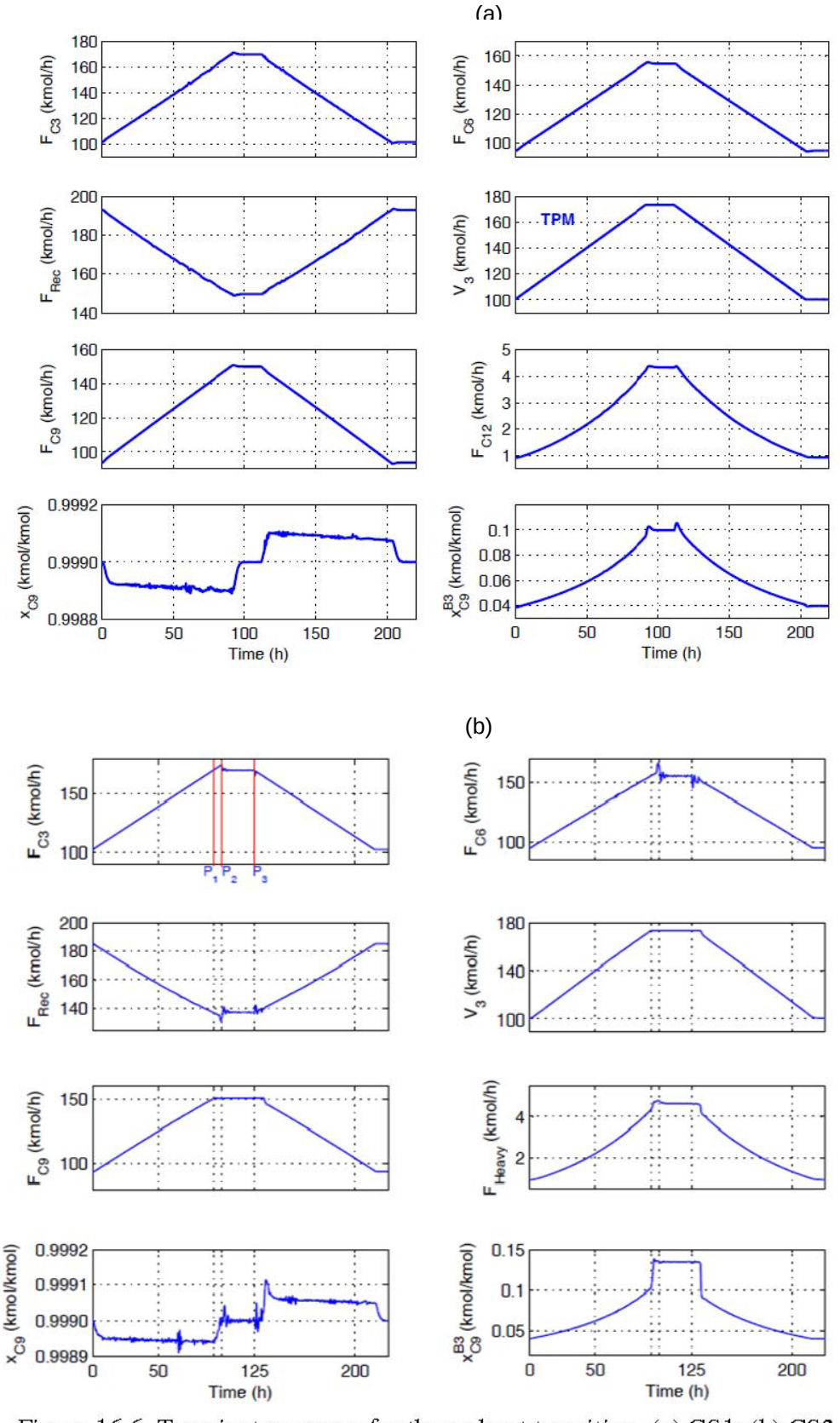

Figure 16.6. Transient response for throughput transition. (a) CS1; (b) CS2

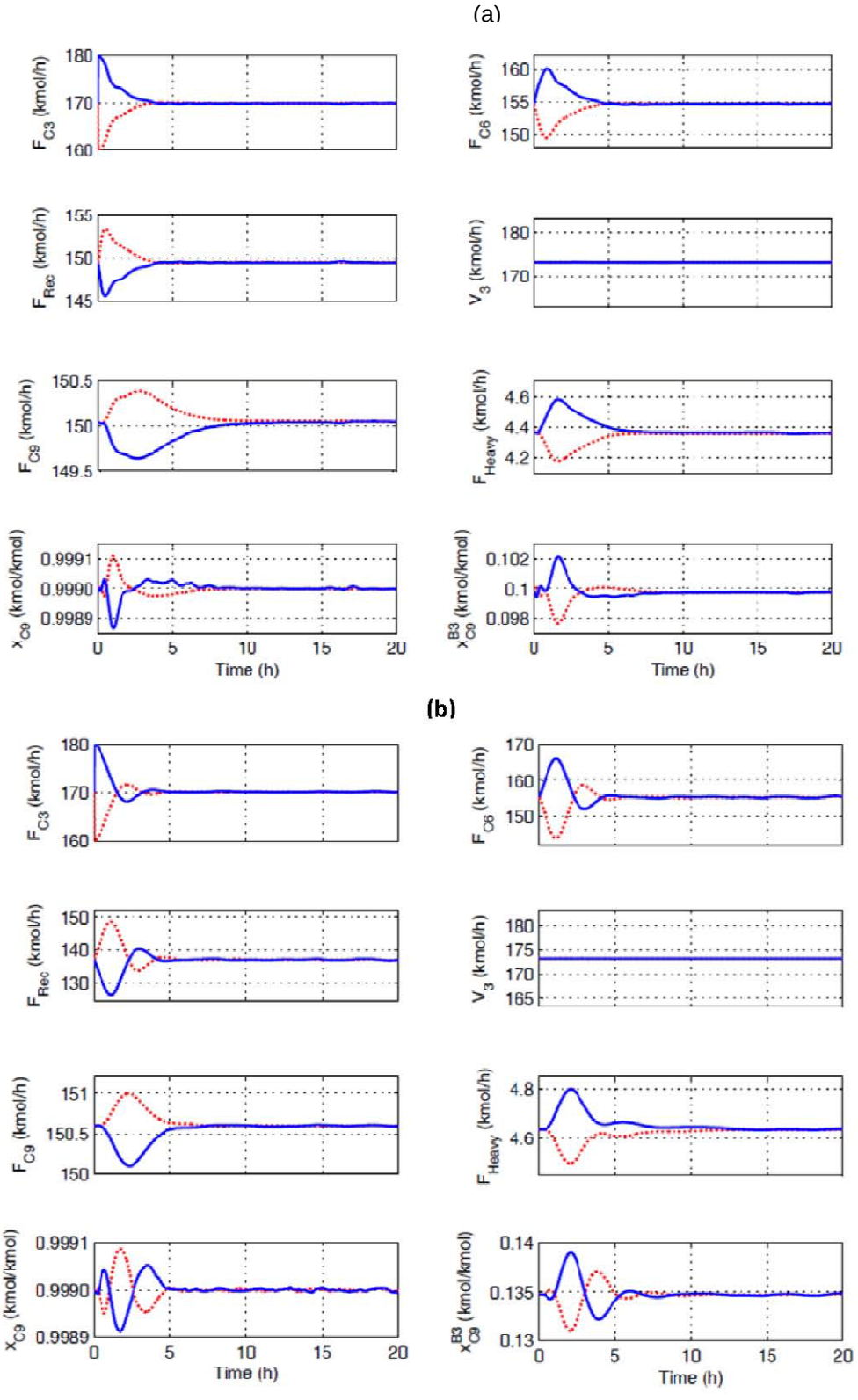

Figure 16.7. Maximum throughput transient response to ±5% step bias in F_{C3} sensor .
(a) CS1; (b) CS2 —: -5% bias;
⋯: +5% bias

(a)

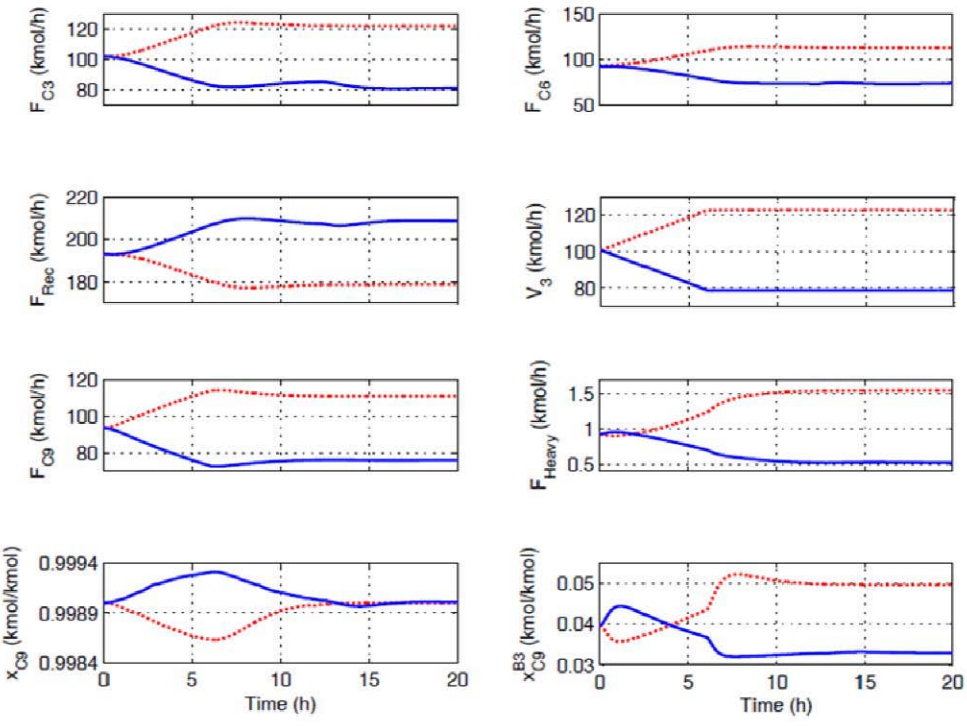
F_C3 (kmol/h)
120
100
80
F_C6 (kmol/h)
150
100
50
F_Rec (kmol/h)
220
200
180
V_3 (kmol/h)
120
100
80
F_C9 (kmol/h)
120
100
80
F_Heavy (kmol/h)
1.5
1
0.5
x_C9 (kmol/kmol)
0.9994
0.9989
0.9984
0
5
10
15
20
Time (h)
x^B3_C9 (kmol/kmol)
0.05
0.04
0.03
0
5
10
15
20
Time (h)

(b)

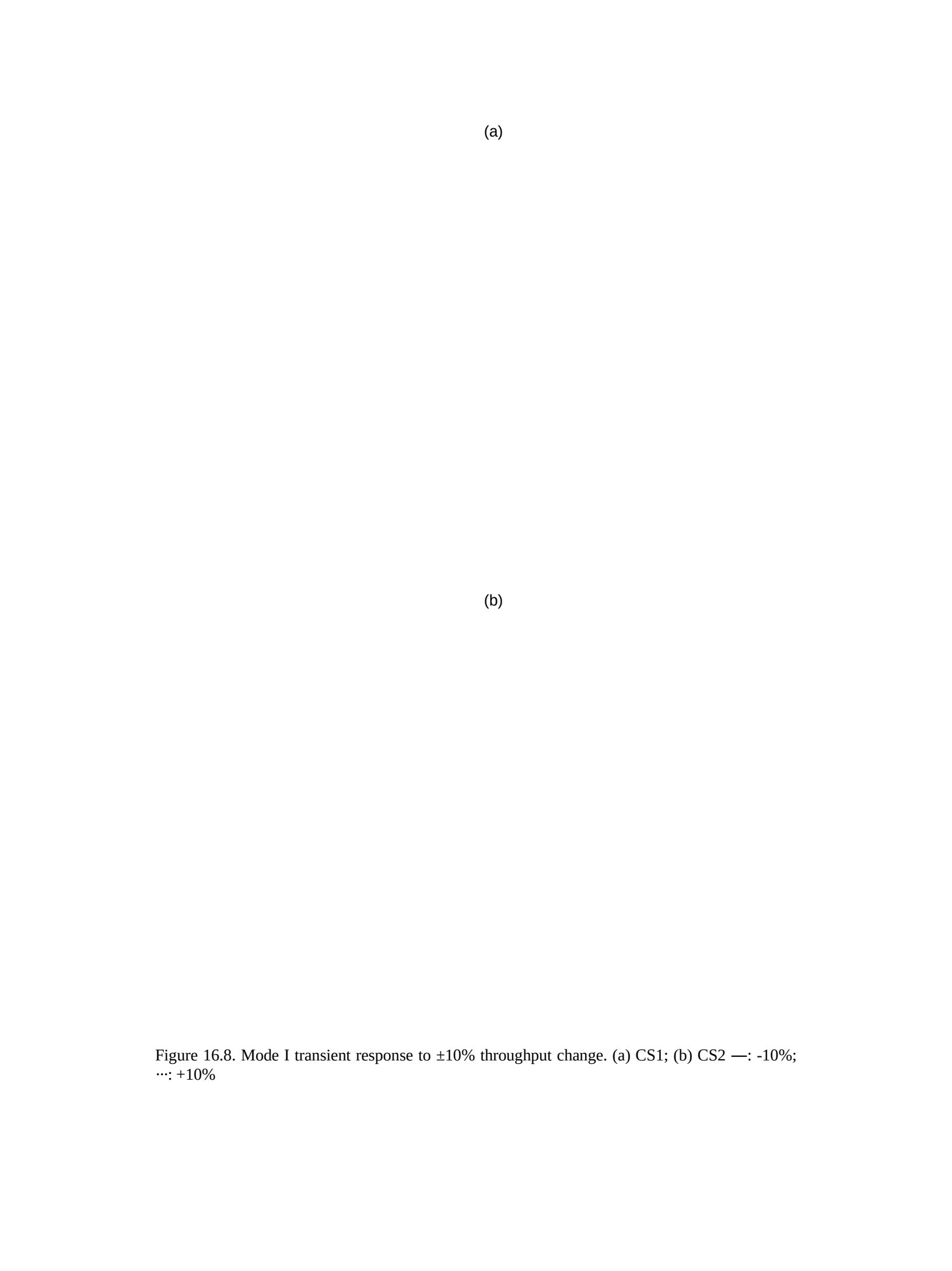

Figure 16.8. Mode I transient response to ±10% throughput change. (a) CS1; (b) CS2 —: -10%; ···: +10%

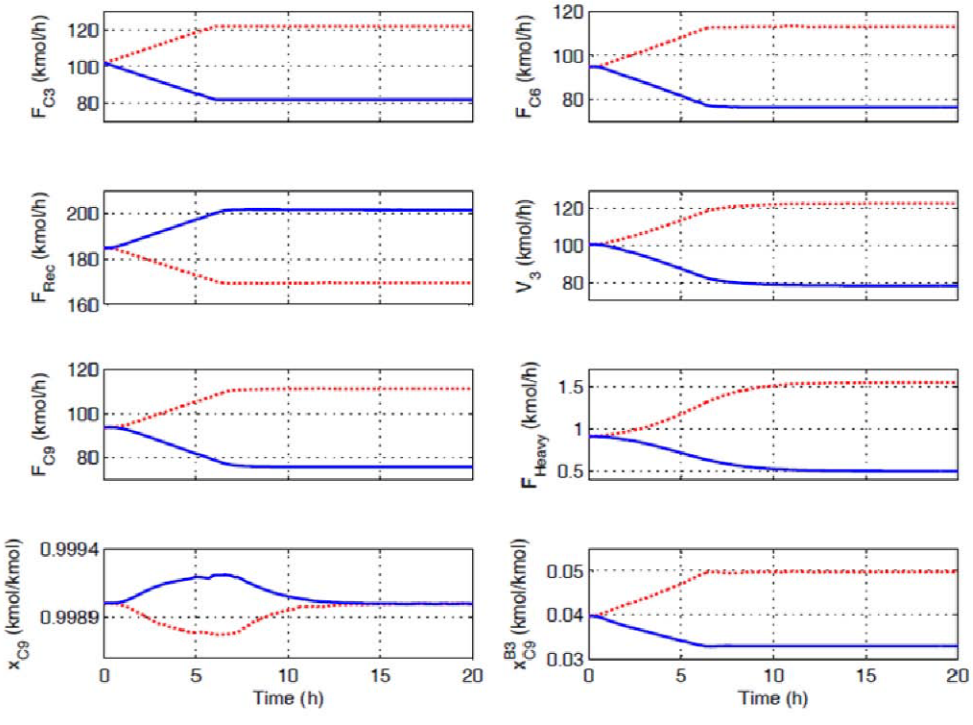

Figure 16.8. Mode I transient response to ±10% throughput change. (a) CS1; (b) CS2
—: -10%; ⋯: +10%

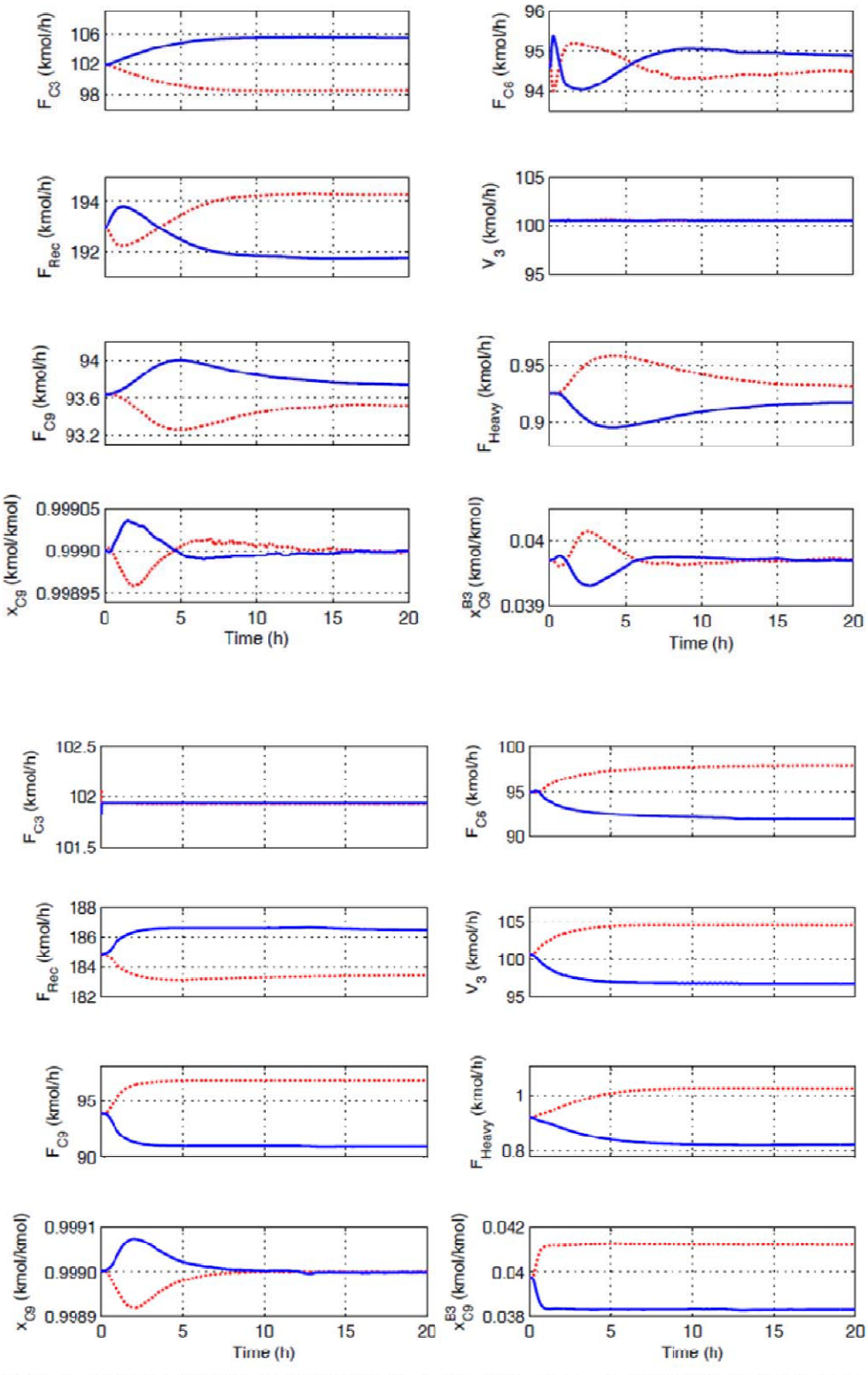

Figure 16.9. Mode 1 transient response to ±3% step in F_{C3} propylene mol fraction.

(a) CS1; (b) CS2

—: -3% ; ···: +3%

16.4.3. Quantitative Dynamic and Economic Comparison of CS1 and CS2

In this subsection, the dynamic and economic performance of CS1 and CS2 is quantitatively compared. In addition to the disturbance scenarios already considered, we consider a -5% step bias in F_{C3} measurement with the initial steady state corresponding to V_3 -V_3^{MAX} approaching 0 (Mode II). The overrides in CS2 are then 'ready to be triggered'.

To quantify the dynamic performance, the IAE values for x_{C9} and $x_{C9}^{D3,B3}$ for the 10h transient period post disturbance are reported in Table 16.5. From the data, it is evident that both structures provide comparable regulation of product purity and the cumene loss in the byproduct stream in Mode I (V_3^{MAX} inactive) for a feed propylene composition change. For a ramped throughput change, even as the regulation of x_{C9}^{B3} is significantly poorer in CS1, it is acceptably

small. As already noted, the larger $x_{C9}^{B3,SP}$ variability in CS1 is because the CS1 TPM (V_3) is located at the product column. The Mode I throughput change data (row 1) also suggests that CS2 achieves slightly tighter product purity control. For Mode II operation, the data (rows 3 and

4) suggests that CS1 and CS2 provide comparable dynamic regulation of x_{C9} and $x_{C9}^{D3,B3}$ for process feed disturbances, namely, a 3% step change in the propylene feed composition or a 5% step bias in the F_{C3} sensor. The IAE values for x_{C9}^{B3} with the T_{Col3}^{S} override about to be triggered (last two rows) with and without external reset suggest that Shinskey's simple external reset scheme significantly improves the tightness of control by ensuring that the unselected output does not deviate too far away from the selected output due to reset windup.

Table 16.5. IAE values for $x_{C9}^{D3,B3}$ for 10 h transient post disturbance

i	Reaction	k_i	$E_{a\,i}$ (kJ/kmol)	Concentration terms $f_i(C_j)$
1	$C_6H_6 + C_3H_6 - C_9H_{12}$	2.8 x 10^7	104174	$C_{C3}C_{C6}$
2	$C_9H_{12} + C_3H_6 - C_{12}H_{18}$	2.32 x 109	146742	$C_{C3}C_{C9}$

Objective	Maximize(J) J: hourly operating profit *	
Process Constraints	*0 ≤ Material Flows ≤ 2 (base case) 0 ≤ V_1, V_2, V_3 ≤ 1.5 (base case) Vent Temperature = 32 ^oC 0 ≤ Energy Flows ≤ 1.7 (base case) 1 bar ≤ P_{Rxr} ≤ 25 bar Cumene Product Purity ≥ 0.999 mol fraction*	
Decision Variable	Mode I	Mode II
$FC3$	101.93 kmol/h Fixed	169.96 kmol/h
$F_{C6\ Total}$	294.16 kmol/h	316.2 kmol/h
$Trxr$	322.26 °C	318.58 °C
$TRxrShell$	368.95 °C	367.98 °C
$PRxr$	25 bar Max	25 bar Max
$Tcooler$	100 °C Fixed	100 °C Fixed
$T_{vent\ D1}$	32 °C Fixed	32 °C Fixed
$x_{C3\ B1}$	0.1 % Fixed	0.1 % Fixed
$x_{C9\ D2}$	0.4 % Fixed	0.4 % Fixed

*: Initial steady state &: TPM setpoint ramped over 0.5 h IAE calculated over 15 h period #: CS2 overrides are 'ready to be triggered' %: No external reset in CS2 T_{pur}^{S} override @: External reset in CS2 T_{pur}^{S} override

To quantify the economic performance, the Mode I and Mode II steady state hourly profit is reported in Table 16.6. In CS2, V_2 is backed-off from $V_2^{SP,MAX}$ by the least amount for which the V_2^{MAX} constraint does not get violated for the worst-case disturbance scenario, which is a -5% step bias in F_{C3}, requiring the maximum back-off from V_2^{MAX}. Negligible back-off is needed in

CS1 which is designed for process operation at V_2^{MAX}. Due to the back-off from V_2^{MAX} in CS2, its steady profit is slightly lower (up to >0.1% in Mode II) than CS1.

Table 16.6. Steady state and transient profit data for CS1 and CS2

Steady state hourly profit data

i	Reaction	k_i	$E_{a\,i}$ (kJ/kmol)	Concentration terms $f_i(C_j)$
1	$C_6H_6 + C_3H_6 \text{-} C_9H_{12}$	2.8 x 10^7	104174	$C_{C3}C_{C6}$
2	$C_9H_{12} + C_3H_6 \text{-} C_{12}H_{18}$	2.32 x 10^9	146742	$C_{C3}C_{C9}$

Transient profit data (IE_P^{Av} and ΔIE_P^{Av} values)

i	Reaction	k_i	$E_{a\,i}$ (kJ/kmol)	Concentration terms $f_i(C_j)$
1	$C_6H_6 + C_3H_6 \text{-} C_9H_{12}$	2.8 x 10^7	104174	$C_{C3}C_{C6}$
2	$C_9H_{12} + C_3H_6 \text{-} C_{12}H_{18}$	2.32 x 10^9	146742	$C_{C3}C_{C9}$

Objective	Maximize(J) J: hourly operating profit *	
Process Constraints	*0 ≤ Material Flows ≤ 2 (base case) 0 ≤ V_1, V_2, V_3 ≤ 1.5 (base case) Vent Temperature = 32 ^{o}C 0 ≤ Energy Flows ≤ 1.7 (base case) 1 bar ≤ P_{Rxr} ≤ 25 bar Cumene Product Purity ≥ 0.999 mol fraction*	
Decision Variable	Mode I	Mode II
F_{C3}	101.93 kmol/h Fixed	169.96 kmol/h
$F_{C6\,Total}$	294.16 kmol/h	316.2 kmol/h
T_{rxr}	322.26 °C	318.58 °C
$T_{RxrShell}$	368.95 °C	367.98 °C
P_{Rxr}	25 bar Max	25 bar Max
T_{cooler}	100 °C Fixed	100 °C Fixed
$T_{vent\,D1}$	32 °C Fixed	32 °C Fixed
$x_{C3\,B1}$	0.1 % Fixed	0.1 % Fixed
$x_{C9\,D2}$	0.4 % Fixed	0.4 % Fixed
$x_{C6\,B2}$	0.09 %	0.05 %
$x_{C9\,D3}$	99.9 % Min	99.9 % Min
$x_{C9\,B3}$	0.4 %	10 %
Optimum J, F_{C9} Active	[illegible]	[illegible]

*: Initial steady state &: TPM setpoint ramped over 6 h. IAE calculated over 15 h period #: CS2 overrides are 'ready to be triggered'

%: No external reset in CS2 T^S_{pur} override

@: External reset in CS2 T^S_{pur} override

To quantify economic losses during transients, Table 16.6 also reports the time average integral error for the 10 hour transient period (T) post disturbance defined as

$$IE_P^{Av} = \frac{\int_0^T \left(P_t - P_f^{SS}\right) dt}{T}$$

where P_t is the instantaneous hourly profit and P_f^{SS} is the final steady state hourly profit for a disturbance. The metric is thus the time average cumulative transient profit deviation from the final steady state profit. Positive (negative) values indicate the extra hourly profit (loss) over the final steady state profit in the transient period. One would expect that any transient profit for a disturbance in one direction would be nullified by a similar transient loss for the same disturbance in the opposite direction. The IE_P^{Av} values for a given disturbance in either direction should thus be approximately the same magnitude but opposite signs. A large negative difference between the two corresponds to an unrecoverable transient economic loss. Table 16.6 also reports this difference

$$\Delta IE_P^{Av} = IE_P^{Av+} - IE_P^{Av-}$$

where IE_P^{Av+} and IE_P^{Av-} correspond to an increase and decrease, respectively, in the disturbance magnitude. As expected, in all but one disturbance scenario, ΔIE_P^{Av} is small for both CS1 and CS2. For a ±5% step change in the F_{C3} measurement with the CS2 overrides 'ready-to-betriggered', the ΔIE_P^{Av} is large negative implying significant unrecoverable transient losses. These losses are attributed to the excessive leakage of precious cumene in B_3 between V_3^{MAX} going active and T_S^{Col3} override taking over B_2 manipulation. Every extra mol of lost cumene consumes expensive reactants that cost twice the product to raw material price difference. Regardless of whether external reset is used or not on the T_S^{pur} override, the transient profit loss is significant at >4.5% of the steady state Mode II profit. The transient loss figures with and without external reset are comparable as the oscillatory x_{C9}^{B3} response for the no external reset leads to cancellation of errors in the undershoots and overshoots.

If the CS2 overrides are switched off (e.g. by an operator), F_{C3}^{SP} must be sufficiently reduced from the maximum achievable throughput so that the V_3^{MAX} constraint does not get violated during the worst-case transient, which is a -5% step change in the F_{C3} measurement. This back-off results in a significant steady hourly profit loss of >4% due to lower maximum throughput. The results demonstrate that CS2 with overrides or backed-off operation results in non-negligible economic loss.

16.4.4. Discussion

The results for the case study suggest that the economic plantwide control structure, CS1, designed for tightest possible control of the economically important hard active constraints (V_3^{MAX} and V_2^{MAX}), achieves superior economic process operation particularly in Mode II, compared to the conventional control structure, CS2. CS1 is also simpler than CS2 in that the inventory management strategy remains fixed regardless of whether the V_3^{MAX} constraint is active or not. CS2 on the other hand is more complicated requiring 3 additional override controllers to alter the material balance control structure all the way up to the C_3 feed, once the V_3^{MAX} constraint goes active. Proper tuning and setpoint selection of these override controllers is necessary to ensure that they get activated in the proper order without too much time elapsing between when V_3^{MAX} goes active and the overrides 'take-over' control. Proper design of the override scheme can be tricky and for severe enough transients, the correct override order may get violated and large plantwide transients can occur due to the overrides 'taking-over' and 'giving-up' control, similar to 'on-off' control. One such occurrence and operators would be inclined to turn the scheme off and resort to the more conservative backed-off process operation with a significantly more severe economic penalty.

It is also worth noting that in our analysis, we have considered only a single disturbance to be active at a time and the hard maximum boilup constraints (V_2^{MAX} and V_3^{MAX}) to be constant. In practice, multiple disturbances are active all the time. More importantly, the hard maximum boil-up constraint limits themselves are transient, depending on the feed flow and reflux flow as well as other factors such as impurities that build-up over time inside the column. The CS2 economic performance is therefore likely to be significantly inferior to CS1 due to the need for a higher back-off in V_2^{MAX} as well as unrecoverable transient cumene loss in the DIPB stream with the override scheme switching on and off due to variability in the V_3^{MAX} limit.

The major difference between CS1 and CS2 is in the location of the TPM; V_3^{SP} for CS1 and F_{C3}^{SP} for CS2. Since V_3 is the last constraint to go active (i.e. the bottleneck constraint) and

also economically important with any back-off resulting in reduced throughput, it makes sense to use it as the TPM and not for the conventional control task of tray temperature control. Typically, due to the high sensitivity of recycle flows to throughput changes (snowball effect), the bottleneck constraint is usually inside the recycle loop. The case study results support the heuristic of locating the TPM at the bottleneck constraint for economic operation.

Lastly, we highlight that the conventional practice in control structure design is to implement inventory control loops with their MVs being 'local' to the specific unit containing the inventory. The basic idea is to ensure that the inventory loops are robust. This case study illustrates that it is possible to develop control structures with seemingly unworkable 'long' inventory control loops that provide acceptable regulation with tight control of the economic CVs over the entire throughput range. The top-down pairing philosophy, as illustrated here should be applied to come up with such unconventional but workable economic plantwide control structures, in the knowledge that should the inventory control be fragile, the pairings can always be revised towards 'local' inventory loops and 'long' economic loops in lieu.

16.5. Conclusions

In conclusion, this article demonstrates through a case-study, the crucial role of economically important maximum throughput hard active constraints in determining the input-output pairings for economic plantwide control. The approach demonstrated here leads to a simple control structure with unconventional inventory loops for process operation over the entire throughput range. Conventional control systems that do not take into consideration the active constraints on the other hand must resort to complicated overrides for constraint handling at high throughputs, with overall inferior economic performance.

Chapter 17. C_4 Isomerization Process

17.1. Process Description

Figure 17.1 shows a schematic of the C_4 isomerization process studied in this work. A fresh C_4 stream containing n-C_4 and i-C_4 with some C_3 and i-C_5 impurities is fed to a deisobutanizer (DIB) column that recovers i-C_4 with some n-C_4 (heavy key) impurity as the distillate. All the C_3 in the fresh C_4 feed leaves in the distillate. The DIB bottoms consisting of nC_4, i-C_5 and some i-C_4 (light key) impurity is fed to a purge column that recovers i-C_5 with some n-C_4 (light key) as the bottoms. The purge column distillate consisting of C_4's and some i-C_5 (heavy key) is fed to an adiabatic packed bed reactor (PBR) after preheating in a feed effluent heat exchanger (FEHE) followed by heating to the reaction temperature in a heater. The n-C_4 isomerizes in the PBR to i-C_4. The hot reactor effluent preheats the cold reactor feed in the FEHE and is then condensed in a flooded cooler. The subcooled liquid is rich in i-C_4 and is fed to the DIB column above the relatively i-C_4 lean fresh C_4 feed. The base-case process design and steady state operating conditions (adapted from Luyben et al.[17]) are shown in Figure 17.1. The irreversible reaction kinetic model in their work is used along with the SRK equation of state to model the thermodynamic properties. Aspen Hysys is used for steady state and dynamic process simulation. Hysys uses the sequential approach for steady state solution of flowsheets with Wegstein updation at the recycle tear. The inside-outside algorithm is used on the distillation columns with the light key and heavy key impurity mol fractions in respectively the bottoms and distillate as the 2 column specifications. For robust recycle-tear convergence, the total benzene flow (recycle + fresh) is specified so that the fresh benzene gets calculated at the end of each recycle tear iteration.

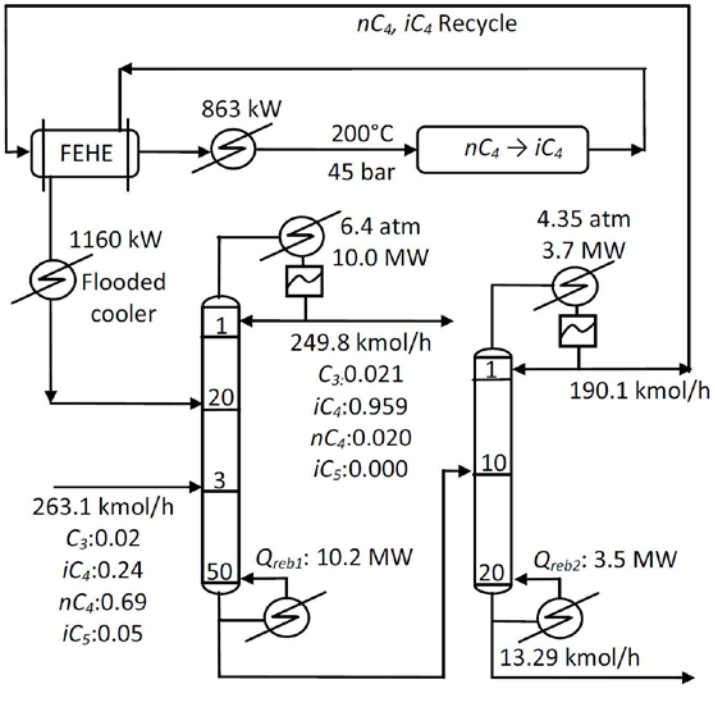

Figure 17.1. Isomerization process schematic with salient design and base operating conditions

17.2. Economic Plantwide Control System (CS1) Design

17.2.1. Step 0: Active Constraint Regions and Economic Operation

The process has 14 independent control valves. Of these, 4 valves must be used to control surge levels, namely, two reflux drum levels and two sump levels on the columns. Also, two valves will get used to maintain the columns at their design pressures There are then 8 steady state operating dofs for the process; 1 for the fresh feed, 2 each for the two columns, 1 for the reactor feed heater, 1 for the reactor effluent cooler and 1 for the reactor pressure. For robust flowsheet convergence, the chosen 8 specification variables are: the fresh C_4 feed (F_{C4}), the DIB

distillate *n*-C_4 and bottoms *i*-C_4 mol fractions (x_{nC4} and $x_{iC4}^{D1\ B1}$), the purge column distillate *i*-C_5 $^{D2\ B2}$
and bottoms *n*-C_4 mol fractions (x_{iC5} and x_{nC4}), the reactor inlet temperature (T_{rxr}) and pressure (P_{rxr}) and the cooler outlet temperature (T_{cool}).

Of the 8 steady state dofs, T_{rxr} and P_{rxr} are assumed fixed at their design values and not considered for optimization. This is done as the kinetic parameters were adapted by Luyben et al.[17] to match the operating conditions of an existing industrial reactor and are therefore artificial. Also, in industrial processes, gas phase reactors are usually operated at the design pressure and not lower so the reaction kinetics are as fast as possible. Also there is usually a very limited recommended catalyst temperature range for which the technology licensor guarantees catalyst life. Holding reactor temperature and pressure constant is therefore a reasonable assumption. The remaining 6 dofs can and should be adjusted for optimizing an economic criterion such as the steady hourly profit or steam consumption per kg product etc. We consider two process operation modes; Mode I where the throughput is fixed (eg by market demand-supply considerations) and Mode II where the market conditions are such that it is optimal to operate the process at maximum throughput.

For Mode I, the optimized economic criterion is the yearly profit, P, defined as
P = [Product Sale – Raw Material Cost – Energy Cost] per year. The fresh C_4 feed (F_{C4}) is fixed at its base case design value (263.1 kmol/h) and the remaining 5 dofs are to be optimized. For Mode II, the objective is to maximize F_{C4} using all 6 dofs (including F_{C4}) as decision variables. The optimization is performed subject to process constraints on the maximum and minimum material / energy flows, maximum column boilup, maximum product impurity and the maximum allowed reactor temperature.

To simplify the optimization, engineering common sense is applied to reduce the number of decision variables. To minimize the loss of precious *n*-C_4 down the purge column bottoms, x_{nC4}^{B2} is chosen to be small at 1% (base-case design value). In addition, the maximum product
impurity constraint ($x_{nC4}^{D1\ MAX}$) should be active for no product give-away. Finally, the cooler outlet temperature, T_{cool}, has almost no impact on the economic objective function and is therefore fixed at a reasonable value of 53 ºC to ensure the reactor effluent vapor is fully condensed using cooling water. These simple engineering arguments leave 2 decision variables,

x_{iC4} and $x_{iC5}^{B1\ D2}$, for Mode I (F_{C4} given) optimization. In Mode II (maximum F_{C4}), F_{C4} is an additional third decision variable.

The optimization is performed using the *fmincon* subroutine in Matlab with AspenHysys 2006 as the background steady state flowsheet solver. The optimization problem formulation and its results are summarized in Table 17.1. In Mode I, the specified F_{C4}, x_{nC4}^{B2} , T_{cool} , T_{rxr} and P_{rxr}
values along with $x_{nC4}^{D1\ MAX}$ active constraint leaves two unconstrained steady state dofs $^{B1\ D2}$
corresponding to x_{iC4} = 0.0565 and x_{iC5} = 0.02. To maximize throughput (Mode II), these two

unconstrained dofs along with the additional dof corresponding to F_{C4} are exhausted to drive the maximum preheater duty (Q_{htr}), maximum purge column boilup (V_2) and maximum *DIB* boilup (V_1) constraints active. At maximum throughput, all steady state dofs get exhausted.

Table 17.1. Isomerization process optimization summary

i	Reaction	k_i	Eu_i (kJ/kmol)	Concentration terms $f_i(C_j)$
1	$C6H6 + C_3H_6 - C_9H_{12}$	2.8 x 10^7	104174	$C_{C3}C_{C6}$
2	$C_9H_{12} + C_3H_6 - C_{12}H_{18}$	2.32 x 109	146742	$C_{C3}C_{C9}$

Objective	Maximize(J) J: hourly operating profit *	
Process Constraints	$0 \le$ Material Flows ≤ 2 (base case) $0 \le V_1, V_2, V_3 \le 1.5$ (base case) Vent Temperature = 32 ^oC $0 \le$ Energy Flows ≤ 1.7 (base case) 1 bar $\le P_{Rxr} \le$ 25 bar Cumene Product Purity ≥ 0.999 mol fraction	
Decision Variable	Mode I	Mode II
$FC3$	101.93 kmol/h Fixed	169.96 kmol/h
$F_{C6\ Total}$	294.16 kmol/h	316.2 kmol/h
$Trxr$	322.26 °C	318.58 °C
$TRxrShell$	368.95 °C	367.98 °C
$PRxr$	25 bar Max	25 bar Max
$Tcooler$	100 °C Fixed	100 °C Fixed
$T_{vent\ D1}$	32 °C Fixed	32 °C Fixed
$x_{C3\ B1}$	0.1 % Fixed	0.1 % Fixed
$x_{C9\ D2}$	0.4 % Fixed	0.4 % Fixed
$x_{C6\ B2}$	0.09 %	0.05 %
$x_{C9\ D3}$	99.9 % Min	99.9 % Min
$x_{C9\ B3}$	0.4 %	10 %
Optimum J F_{C9} Active Constraints	\$3.809x10_3 h $^{-1}$ 93.59 kmol/h $x_{C9\ D3\ MIN}$, $P_{Rxr\ MAX}$, $V_{2\ MAX}$	\$5.879x10_3 h $^{-1}$ 150.045 kmol/h $x_{C9\ D3\ MIN}$, $P_{Rxr\ MAX}$, $V_{2\ MAX}$, $V_{3\ MAX}$

SNo	*CV*	*Remarks on regulatory / economic significance*
1	F_{C3}	Determines process throughput. Maximum throughput limited by $V_{3\ MAX}$
2	$F_{C6\ Total}$	Increasing F_{C6Tot} improves selectivity. Maximum F_{C6Tot} limited by $V_{2\ MAX}$. Affects reactor conversion and selectivity

*: Heater duty \$9.83 GJ; Steam \$4.83 GJ; Cooling water \$0.16 GJ; F_{C4} \$ 32.5kmol; F_{iC4} \$ 42.0kmol; F_{iC5} \$ 22.0kmol $^{-1}$ &: F_{C4} is specified ; ^: Active constraint; #: F_{C4} is optimized for maximum throughput

As the throughput is increased from Mode I (F_{C4} = 263.1 kmol/h), the optimization of the two unconstrained dofs using *fmincon* shows that Q_{htr}^{MAX} is the first constraint that becomes active at an F_{C4} of about 320 kmol/h. A further increase in throughput to 334 kmol/h F_{C4} drives V_1^{MAX} active followed by V_2^{MAX} becoming active at the maximum throughput of 334.5 kmol/h. The increase in throughput over what is achieved when Q_{htr}^{MAX} becomes active is quite small at ~4.5%. We therefore assume that once Q_{htr}^{MAX} becomes optimally active, incrementally higher throughput is achieved by driving V_1^{MAX} and V_2^{MAX} constraints active. The large throughput range from 263.1 kmol/h to the maximum throughput of 334.5 kmol/h witnesses Q_{htr}^{MAX}, V_1^{MAX} and V_2^{MAX} becoming active. These constraints are in addition to $_{D1\ MAX\ B2}$ the other always active constraint x_{nC4} and specifications for T_{rxr}, P_{rxr}, T_{cool} and x_{nC4}, the latter specification being economically significant. If we assume that Q_{htr} is adjusted for a desired reactor inlet temperature of T_{rxr}, then once the Q_{htr}^{MAX} constraint becomes active at a high throughput, a further increase in throughput is made possible by reducing the i-C_5 leaking up the purge column distillate and the i-C_4 leaking down the DIB column distillate. The reduced i-C_4/C_5

circulating around the plant causes the flow through the reactor to reduce allowing more F_{C4} to be processed while keeping the Q_{htr}^{MAX} constraint active.

17.2.2. Step 1: Loops for Tight Economic CV Control

At maximum throughput, Q_{htr}^{MAX}, V_1^{MAX} and V_2^{MAX} are process inputs (potential MVs) constrained to be active. These are hard active constraints and back-off in these must be minimized for process operation at the maximum possible throughput. In addition, $x_{nC4}^{D1\,MAX}$ constraint, which is a process output (CV), is active along with output specifications for T_{rxr}, P_{rxr}, $x_{nC4}^{B2\,D1MAX\,B2}$ and T_{cool}. Of these, tight control of x_{nC4}^{B2} and x_{nC4}^{D1} is desirable for respectively, on-aim product quality and small loss of precious *n*-C_4 in the purge column bottoms. The analytical measurement x_{nC4}^{B2} is not related to the product quality and therefore unlikely to be available in practice. As the purge column temperature profile is quite sharp, the average temperature of sensitive stripping tray temperatures, $T_{pur}^{S\,thth}$ (14-16tray from top) is therefore controlled as an inferential measure of x_{nC4}^{B2}. Due to their economic significance, we first pair loops for tight control of Q_{htr}^{MAX}, V_2^{MAX}, V_1^{MAX} and x_{nC4}^{D1} at their maximum limits as well as tight control of T_{pur}^{S}.

The Q_{htr}^{MAX} valve is left fully open for process operation at Q_{htr}^{MAX}. For operating the columns close to their maximum boil-up limits (i.e. close to flooding limit) with negligible back-off, the respective reboiler steam valves are used to control the boilups. Thus V_1 is paired with Q_{reb1} and V_2 is paired with Q_{reb2}. Tight control of the product impurity x_{nC4}^{D1} is achieved by manipulating the DIB column reflux (L_1). Because V_2^{MAX} is active, T_{pur}^{S} cannot be controlled conventionally using boilup, V_2, and the feed to the purge column (B_1) is used as the MV instead.

For effective stabilization of the reactor, its pressure and temperature must be controlled tightly. Since Q_{htr}^{MAX} is active, the reactor inlet temperature is maintained at its setpoint using the reactor feed flow stream (D_2). Note that the degree-of-tightness of control in this arrangement would be comparable to Q_{htr} as the MV since the open loop dynamic response time constants are likely to be comparable. The reactor pressure is controlled at its design value by manipulating the cooler outlet valve. To ensure proper condensation of the reactor effluent, the cooler duty (Q_{cool}) is manipulated to maintain T_{cool}.

17.2.3. Step 2: Inventory Control System

We now pair loops for remaining inventories that are not important from the economic standpoint. The two column pressures (P_{col1} and P_{col2}) are controlled at their specified values conventionally using the respective condenser duties (Q_{cnd1} and Q_{cnd2}). Lastly, we pair loops for the four surge levels on the two columns. Since the purge column distillate is already paired with the T_{rxr} controller, its reflux drum level (LVL_{RD2}) is controlled using the reflux rate (L_2). The purge column sump level (LVL_{Bot2}) is controlled using the column bottoms (B_2). Note that even as B_2 is a very small stream, effective level control will be achieved as long as T_{pur}^{S} is controlled, an economic loop already paired. The DIB reflux drum level (LVL_{RD1}) is controlled using the distillate (D_1). Since B_1 is already paired for purge column temperature control, the DIB column sump level (LVL_{Bot1}) is controlled using the fresh C_4 feed (F_{C4}). It is highlighted that in the control structure for maximum throughput operation, the light key *i*-C_4 impurity leaking down the DIB bottoms and the heavy key *i*-C_5 impurity leaking up the purge column distillate are not controlled and float at appropriate values determined by the values of V_1^{MAX} and V_2^{MAX} as well as the other setpoints.

17.2.4. Step 3: Throughput Manipulation and Additional Economic Loops

We now seek an appropriate strategy for reducing throughput while ensuring (near) optimal operation at lower throughputs. From the optimal Mode I and Mode II results in the previous section, V_2 is the last constraint to go active. On reducing throughput, V_1 is the next constraint to go inactive followed by Q_{htr}. The sensitivity of throughput with respect to the constraint variables decreases in order Q_{htr}, V_1 and V_2. As explained previously, once Q_{htr} goes active, only an incremental increase in throughput is achieved by reducing the *i*-C_4 leaking down DIB column (this causes V_1 to go active) and the *i*-C_5 leaking up the purge column (this causes V_2 to go active).

The simplest way to reduce throughput (Option 1) would be to maintain the boilups at V_1 and V_2 and reduce Q_{htr}. Even as throughput would reduce, the operation would be suboptimal due to overrefluxing in the two columns (unnecessarily high boilups). For near optimal operation at low throughputs, this overrefluxing must be mitigated. One simple possibility (Option 2) is to hold V_2 and V_1 in ratio with the respective column feeds, with the Mode I optimum ratio as their setpoint. Another possibility (Option 3) is to hold the difference between two appropriate DIB column stripping tray temperatures ($\Delta T_{DIB} = T_{37} - T_{32}$) constant by adjusting V_1 and holding V_2 in ratio with B_1. The setpoint for these two controllers would be the Mode I optimum value. Note that ΔT_{DIB} is controlled instead of a tray temperature as the DIB temperature profile is quite flat. The last option (Option 4) is to maintain x_{iC4} and x_{iC5} at their Mode I optimum values by adjusting respectively V_1 and V_2. This however requires two additional composition analyzers, an unlikely scenario in an industrial setting.

Figure 17.2 compares the optimum steady state profit at various throughputs with the profit achieved using the four different options: (1) process operation at V_1 and V_2 at all throughputs; (2) $V_1/(F_{C4} + D_2)$ and V_2/B_1 held constant at Mode I optimum till V_1 and V_2 become active; (3) ΔT_{DIB} and V_2/B_1 held constant at Mode I optimum till V_1 and V_2 become active and (4) x_{iC4} and x_{iC5} held constant at its Mode I optimum till V_1 and V_2 become active. Note that for the price data used, the operating profit decreases for a throughput increase beyond F_{C4} ~332 kmol/h. This point then represents an economic bottleneck and one would operate below this throughput. The economic scenario may however change with significantly higher margins for the product, in which case it may become optimal to operate the process at maximum throughput.

Of the various options considered, Option 4 is economically the best with almost no economic loss from optimum till a throughout of F_{C4} ~ 320 kmol/h, where V_1 becomes active. The simpler Option 3 with no additional composition analyzers is comparable to Option 4. The still simpler Option 3 using ratio controllers gives slightly higher profit loss (~1%) at low throughputs. The simplest Option 1 is economically the worst with a significantly higher economic loss between of up to 8% over the throughput range. These results suggest that Option 2 represents a good compromise between simplicity and minimizing the steady state economic loss. It is therefore considered for implementation.

The overall throughput manipulation scheme in Option 2 is then as follows. At low throughputs, Q_{htr} is used as the throughput manipulator (TPM). Once Q_{htr} goes active to increase throughput, throughput manipulation is shifted to ΔT_{DIB}, which must be increased for a higher throughput. Once V_1 goes active, the TPM is shifted to V_2/B_1, which must again be increased to enhance throughput. Once the V_2 limit is reached, the process operates at the maximum achievable throughput. A reverse logic applies for reducing throughput below

maximum. The TPM for the entire throughput range is then a split range controller, its output shifting from Q_{htr}^{SP} to ΔT_{DIB}^{SP} to V_2/B_1 to increase throughput from low to maximum and vice

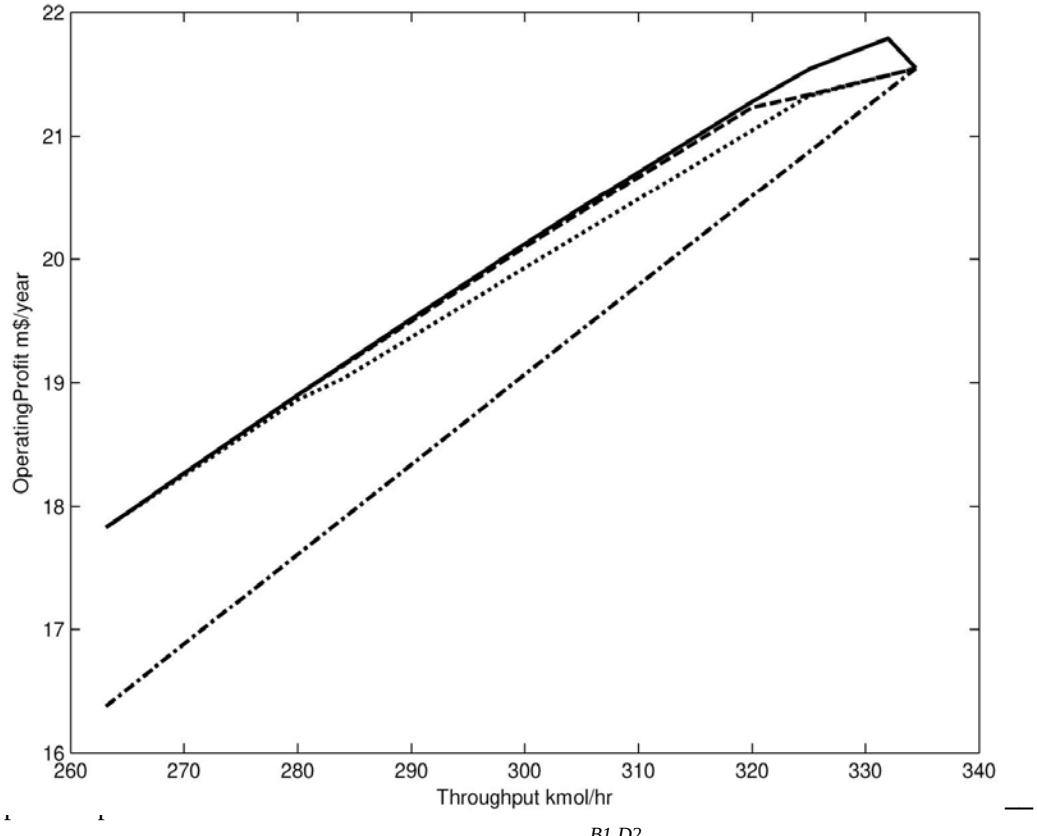

— : Constant x_{iC4} and x_{iC5} $^{B1\ D2}$

• • • • : Constant $V_1/(F_{C4} + D_2)$ and V_2/B_1 $^{MAX\ MAX}$

_ • _ : Process operation at V_1 and V_2

versa. Figure 17.3 depicts the economic plantwide control structure, labeled CS1 for convenient reference, including the split-range throughput manipulation scheme. Note that low and high limits are applied on ΔT_{DIB}^{SP} and V_2/B_1^{SP} for throughput manipulation. The low limit for both corresponds to the Mode I optimum values. The high limits for ΔT_{DIB}^{MAX} and V_2/B_1^{MAX} are chosen slightly above the values for which V_1 and V_2 go active, respectively. In Table 17.2(a), the sequence in which the different pairings are implemented to obtain CS1 is also listed.

17.3. Conventional Plantwide Control Structure (CS2)

Conventionally, the feed to a process is used as the throughput manipulator and the plantwide control system is configured with the inventory control loops oriented in the direction of process flow. Such a TPM choice is often dictated in integrated chemical complexes with the plant feed being set by an upstream process. Figure 17.4 shows such a conventional plantwide control structure, labeled CS2, for the isomerization process. To contrast with CS1, the sequence in which the pairings are obtained for CS2 are noted in Table 17.2(b).

In CS2, the column level and pressure controllers are first implemented along with the reactor pressure and temperature loops (material and energy balance control). On the two

columns, the top and bottom levels are controlled using respectively the reflux and bottoms. The two column pressures are controlled using the respective condenser duties. The reactor inlet temperature is controlled using the furnace duty. The reactor pressure is controlled using the reactor effluent condenser outlet valve while the condensed reactor effluent temperature is controlled using its condenser duty.

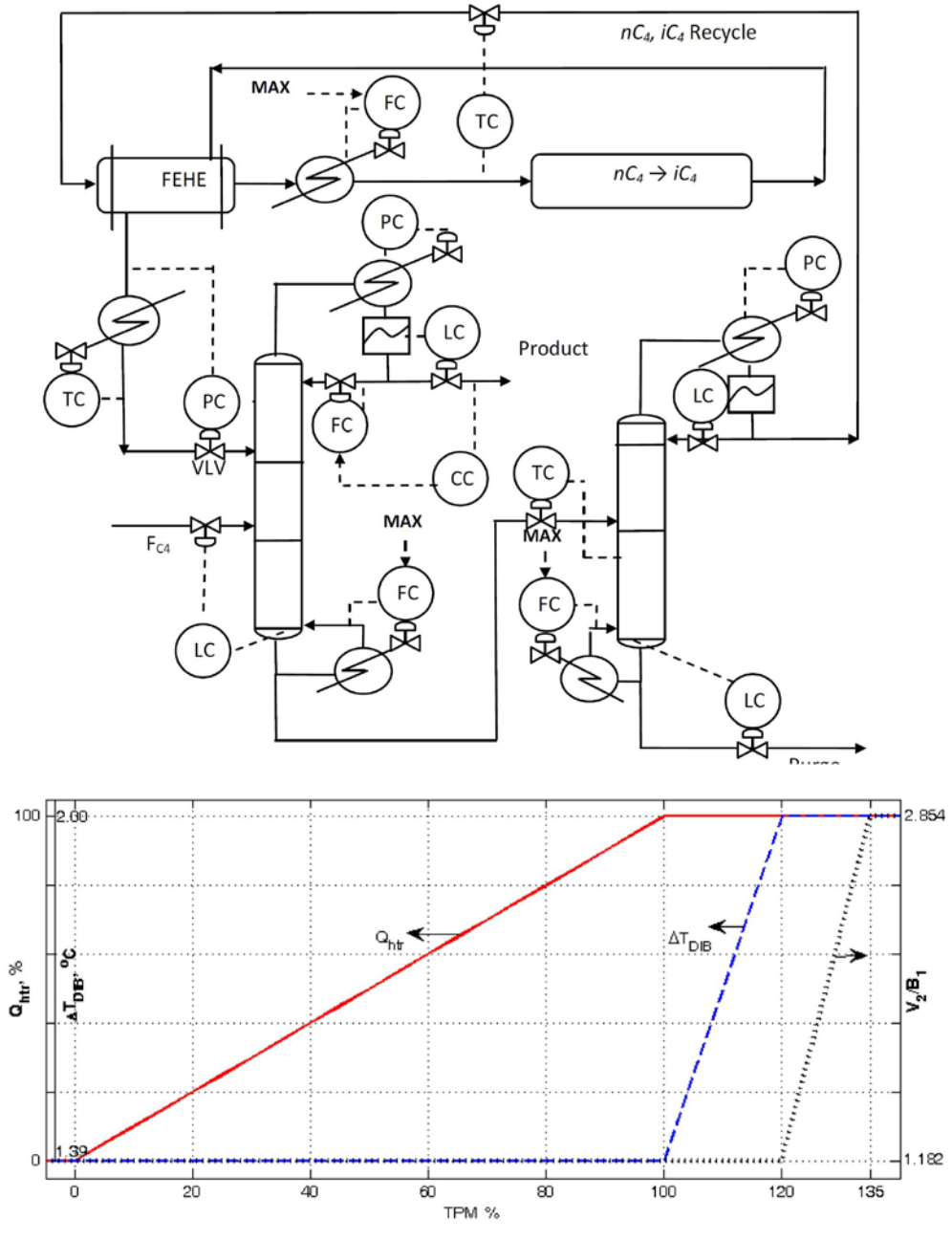

Figure 17.3. Economic Plantwide control structure CS1 with split range throughput manipulator for maximum throughput operation

Table 17.2. Loop pairing sequence followed for CS1 and CS2

i	Reaction	k_i	$E_{a\,i}$ (kJ/kmol)	Concentration terms $f_i(C_j)$
1	$C_6H_6 + C_3H_6 \rightarrow C_9H_{12}$	2.8 x 10^7	104174	$C_{C3}C_{C6}$
2	$C_9H_{12} + C_3H_6 \rightarrow C_{12}H_{18}$	2.32 x 10^9	146742	$C_{C3}C_{C9}$

Objective	Maximize(*J*) *J*: hourly operating profit *	
Process Constraints	*0 ≤ Material Flows ≤ 2 (base case) 0 ≤ V_1, V_2, V_3 ≤ 1.5 (base case) Vent Temperature = 32 °C 0 ≤ Energy Flows ≤ 1.7 (base case) 1 bar ≤ P_{Rxr} ≤ 25 bar Cumene Product Purity ≥ 0.999 mol fraction*	
Decision Variable	Mode I	Mode II
F_{C3}	101.93 kmol/h Fixed	169.96 kmol/h
$F_{C6\,Total}$	294.16 kmol/h	316.2 kmol/h
T_{rxr}	322.26 °C	318.58 °C
$T_{RxrShell}$	368.95 °C	367.98 °C
P_{Rxr}	25 bar Max	25 bar Max
T_{cooler}	100 °C Fixed	100 °C Fixed
$T_{vent\,D1}$	32 °C Fixed	32 °C Fixed
$x_{C3\,B1}$	0.1 % Fixed	0.1 % Fixed
$x_{C9\,D2}$	0.4 % Fixed	0.4 % Fixed
$x_{C6\,B2}$	0.09 %	0.05 %
$x_{C9\,D3}$	99.9 % Min	99.9 % Min
$x_{C9\,B3}$	0.4 %	10 %
Optimum *J* F_{C9} Active Constraints	\$3.809x10^3 h^{-1} 93.59 kmol/h $x_{C9\,D3\,MIN}$, $P_{Rxr\,MAX}$, $V_{2\,MAX}$	\$5.879x10^3 h^{-1} 150.045 kmol/h $x_{C9\,D3\,MIN}$, $P_{Rxr\,MAX}$, $V_{2\,MAX}$, $V_{3\,MAX}$

SNo	CV	Remarks on regulatory / economic significance
1	F_{C3}	Determines process throughput. Maximum throughput limited by $V_{3\,MAX}$
2	$F_{C6\,Total}$	Increasing F_{C6Tot} improves selectivity. Maximum F_{C6Tot} limited by $V_{2\,MAX}$. Affects reactor conversion and selectivity.
3	T_{rxr}	Stabilizes reaction heat recycle through FEHE. Affects reactor conversion

With the basic material/energy balance loops in place, pairings for component inventory control are implemented next. The product nC_4 impurity leaking up the DIB column is controlled by adjusting D_1/L_1. The boilup, V_1, is adjusted to maintain ΔT^S_{DIB}. The purge column distillate is maintained in ratio with its reflux while the bottoms is used control T^S_{pur}. With the T^S_{pur} loop, the small purge column bottoms stream would provide acceptable sump level control. With these pairings, the control structure would provide stable unconstrained operation ie Mode I operation. The operation would be near optimal for appropriate choice of the steady state dof setpoints. Upon hitting constraints such as Q_{htr}^{MAX} on increasing throughput, appropriate overrides are needed to ensure control of crucial CVs is not lost. These overrides are also shown in Figure 17.4 and are briefly explained below.

On increasing the F_{C4} to increase throughput, the $Q_{htr}^{SP\,MAX}$ constraint would be hit implying loss in control of T_{rxr}. Losing T_{rxr} control is not acceptable and an alternative manipulation handle for maintaining T_{rxr} is needed. The closest manipulation handle that would provide tight T_{rxr} control is D_2. An override T_{rxr} controller is therefore implemented with its setpoint slightly below the nominal setpoint. When Q_{htr} is unconstrained, T_{rxr} would be above the override controller temperature setpoint and the override controller output would increase. This output would then be high and the low select block would pass the D_2/L_2 ratio controller output

to D_2 (i.e. D_2^{SP} under ratio control). When $Q_{htr}^{SP\,MAX}$ is hit, T_{rxr} would start decreasing and go below the override controller setpoint, whose output would decrease till the low select ultimately passes this signal to D_2 (i.e. D_2^{SP} under T_{rxr} control).

Figure 17.4. Conventional plantwide control structure, CS2

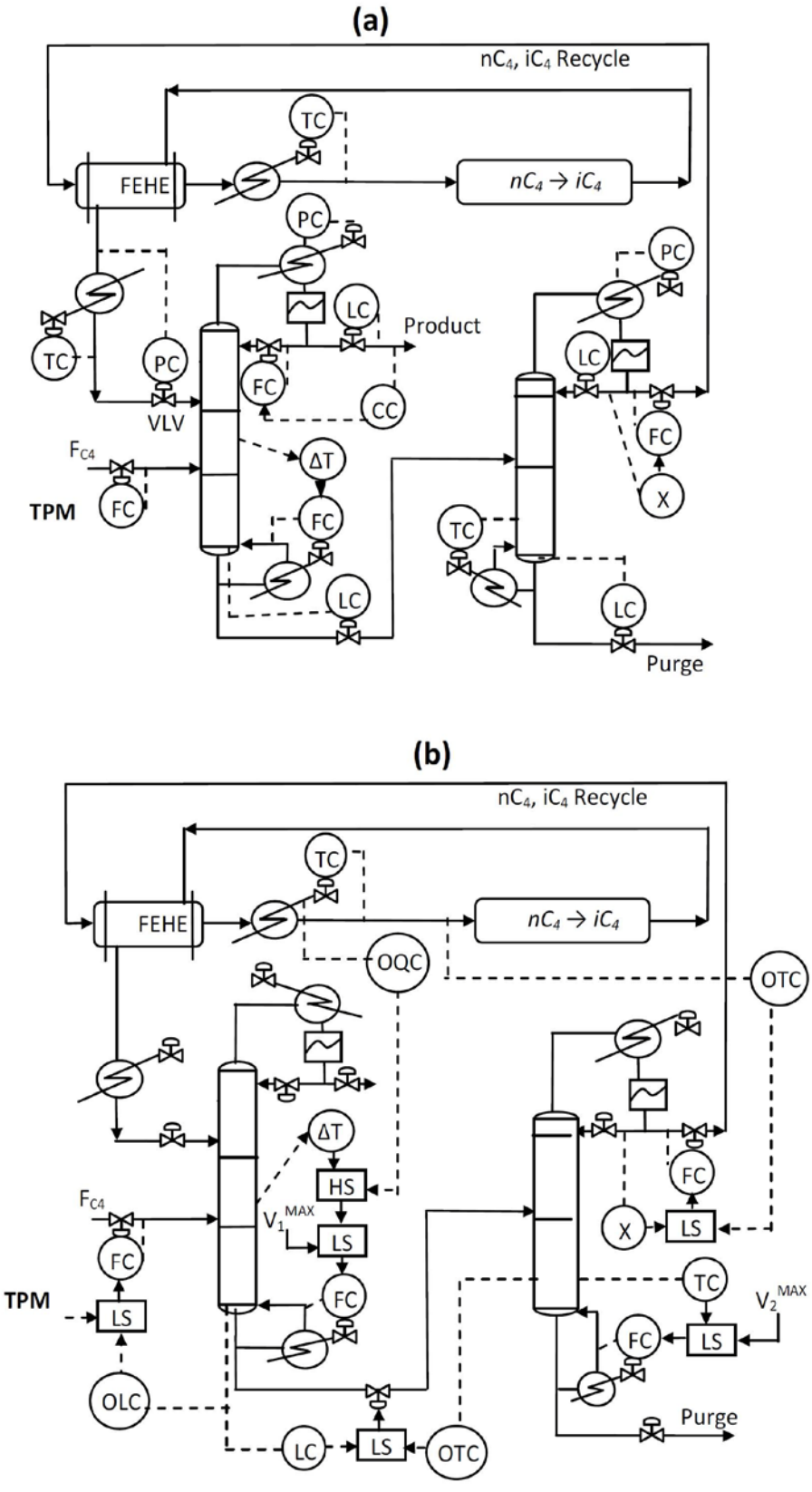

(a) Basic pairings for Mode I (unconstrained) operation
(b) Overrides for handling constraints

It is possible to bring about a near optimal increase in throughput with Q_{hr}^{MAX} active by driving V_1^{MAX} and V_2^{MAX} active, in that order. To do so, a PI Q_{htr} override controller with its setpoint very close to the Q_{htr}^{MAX} limit is implemented. The high select on the Q_{htr} override output and the ΔT_{DIB} controller output, selects the greater of the two signals. The selected signal is sent as the setpoint to the V_1 controller through a low select that ensures V_1 does not ever exceed $V_1^{SP,MAX}$. At low throughputs (F_{C4} low, $Q_{htr} < Q_{htr}^{MAX}$) the direct acting Q_{htr} override controller output would decrease and the high select would pass the ΔT_{DIB} controller output. On sufficiently increasing F_{C4}, Q_{htr} would increase above the override controller setpoint, and the controller output would start to increase. The high select would ultimately pass V_1^{SP} manipulation to the Q_{htr} override, which would cause V_1 to increase. If F_{C4} is high enough (or increased fast enough), V_1 would reach $V_1^{SP,MAXS}$. The T_{pur} controller would increase V_2 to ensure that the *n*-C_4 does not leak out the purge column bottoms. V_2^{MAX} going active would signal that fresh *n*-C_4 beyond the processing capacity of the plant is being fed. To automatically reduce F_{C4} to the maximum processing capacity limit, an override scheme for altering the material balance structure from V_2^{MAX} all the way back to the process fresh feed is implemented.

When $V_2^{MAX,S}$ goes active, T_{pur} control is lost implying excessive leakage of precious *n*-C_4 down the purge column bottoms and consequent economic loss. To prevent the same, an alternative manipulation handle for $T^{S}pur$ is needed. The feed to the purge column would provide reasonably tight tray temperature control. A PI $T^{S}pur$ override controller with its setpoint slightly below the nominal setpoint is implemented. When V_2^{MAX} is inactive, the tray temperature would be higher than the override controller setpoint so that its output would increase. The low select on LVL_{Bot1} controller output and the $T^{S}pur$ override controller output would pass the former signal to B_1 (purge column feed under LVL_{Bot1} control). When V_2 goes active, T_{pur} control would be lost and it would decrease below the override controller setpoint. The controller output would then decrease and the low select would ultimately pass $B_1^{SP,MAX,S}$ manipulation to the override controller (purge column feed under $T^{S}pur$ control). LVL_{Bot1} control is now lost and it would increase. A reverse acting LVL_{Bot1} override controller with a setpoint slightly higher than the nominal setpoint is implemented. As LVL_{Bot1} increases, its output would decrease (reverse action). The low select on this signal and operator specified F_{C4}^{SP} would ultimately pass the former signal as the setpoint to the fresh C_4 feed flow controller causing the fresh feed to be cut by the appropriate amount once V_2^{MAX} goes active. As recommended by Shinskey [21], external reset on all PI controllers whose output passes through a low/high select block is used to ensure that when inactive, the output is not too far from the selected signal due to reset windup. This ensures quick 'taking over' of control so that the duration for which a CV remains unregulated is as small as possible. The external reset is implemented internally in AspenHysys.

17.4. Dynamic Simulations and Closed Loop Results

17.4.1. Tuning of Controllers

The performance of the two control structures, CS1 and CS2, is evaluated using rigorous dynamic simulations in AspenHysys 2006. To ensure that any differences in the performances are largely attributable to the structure, a consistent tuning procedure is followed for tuning the loops in both the structures. All flow controllers are tuned with a gain of 0.5 and a reset time of 0.5 mins. All pressure controllers are tuned for tight pressure control, which is any way necessary for stabilizing the pressure driven dynamic simulation. All level controllers are P only

with a gain of 2. The only exception is the DIB sump level controller in CS1 where a lower gain of 1 is used since the lag between the sump and the fresh C_4 feed is significant due to the intervening 20 stripping trays. In all temperature loops, the temperature measurement is lagged by 1 minute to account for sensor dynamics. Also, the controller output signal is lagged by 2 mins to account for heat transfer equipment dynamics. The only exception is the cooler temperature controller where a higher 8 min lag is applied to account for the slow dynamics of a flooded condenser. All temperature controllers are PI(D) and tuned using the autotuner with minor refinement for a not-too-oscillatory closed loop servo response, if necessary. In the PI product composition control loop, a 5 minute dead time and a 5 minute measurement sampling time is applied. The autotuner does not give reasonable tuning and the open loop step response is used to set the reset time at the 2/3rd response completion time and the controller gain adjusted for a not-too-oscillatory servo response. In both structures, the product composition loop is tuned first with the ΔT_{DIB} loop on manual followed by tuning of the ΔT_{DIB} loop with the composition loop on automatic. This ensures that all the detuning due to multivariable interaction gets taken in the ΔT_{DIB} loop and not the product purity loop. This gives tight product purity control, an economically important control objective.

In the CS2 override scheme, the override setpoint for T_{rxr} and T^{S}_{pur} cannot be chosen too close to the corresponding nominal controller setpoint as that would lead to unnecessary controller output switching during routine transients causing further transients. Accordingly the override controller setpoint is chosen as close as possible to the corresponding nominal controller setpoint for the disturbance that causes the worst-case transients. It is also highlighted that the Q_{htr} override controller that manipulates V_1 is a long loop with slow dynamics. Since its setpoint must be close to Q^{MAX}_{htr}, a P only controller would require a large gain to ensure V_1 gets driven to V_1^{MAX} for achieving maximum throughput. The large gain leads to on-off control for routine disturbances at a high but below maximum throughput with the override taking over and giving up V_1 manipulation. A loose PI Q_{htr} override controller is therefore implemented to ensure its setpoint is close to Q^{MAX}_{htr} and on-off control is avoided. Table 17.3 lists the salient controller tuning parameters for CS1 and CS2 using the above procedure.

Table 17.3. Controller tuning parameters

Regulatory controllers

i	Reaction	k_i	E_{ai} (kJ/kmol)	Concentration terms $f_i(C_j)$
1	$C_6H_6 + C_3H_6 - C_9H_{12}$	2.8 x 10^7	104174	$C_{C3}C_{C6}$
2	$C_9H_{12} + C_3H_6 - C_{12}H_{18}$	2.32 x 109	146742	$C_{C3}C_{C9}$

Objective	Maximize(J) J: hourly operating profit *	
Process Constraints	*$0 \le$ Material Flows $\le$ 2 (base case) $0 \le V_1, V_2, V_3 \le$ 1.5 (base case) Vent Temperature = 32 ^oC $0 \le$ Energy Flows $\le$ 1.7 (base case) 1 bar $\le P_{Rxr} \le$ 25 bar Cumene Product Purity $\ge$ 0.999 mol fraction*	
Decision Variable	Mode I	Mode II

CS2 override controllers

	MV	K_C	τ_i (mins)	SP	Sensor Span
Q_{htr}	V_1	0.05	150	1230kW	0-1294kW
T_{rxr}	D_1	0.4	10	199.5 ^{o}C	160-240 ^{o}C
STpur	B_1	0.5	40	58 ^{o}C	40-80 ^{o}C
LVL_{Bot1}	F_{C4}	2	-70%	0-50%	

17.4.2. Closed Loop Results

The plantwide transient response of the two control structures, CS1 and CS2, is obtained for principal disturbances for Mode I and Mode II operation. In Mode I, a ±5 mol% step change in the fresh C_4 feed *i*-C_4 mol fraction with a complementary change in the *n*-C_4 mol fraction and a ±20 kmol/h F_{C4} (throughput change) are considered the principal disturbances. In Mode II, only the feed composition step change is considered the principal disturbances as the throughput gets fixed by the active constraints. The dynamic response is also obtained for a throughput transition from Mode I to Mode II and back.

Figure 17.5 plots the dynamic response of salient process variables to a feed composition step disturbance in Mode I for CS1 and CS2. Both structures are observed to effectively reject the disturbance with tight control of the *n*-C_4 impurity in the product. In CS1, F_{C4} gets adjusted and the flow to the reactor settles to the appropriate value for maintaining T_{rxr} for the set Q_{htr}, the TPM. In CS2 on the other hand, the F_{C4} (TPM) remains fixed and the *i*-C_4 production changes in proportion to the *n*-C_4 in the fresh feed. In both structures, the leakage of *n*-C_4 down the purge column bottoms is well regulated via the action of the T^{s}_{pur} controller.

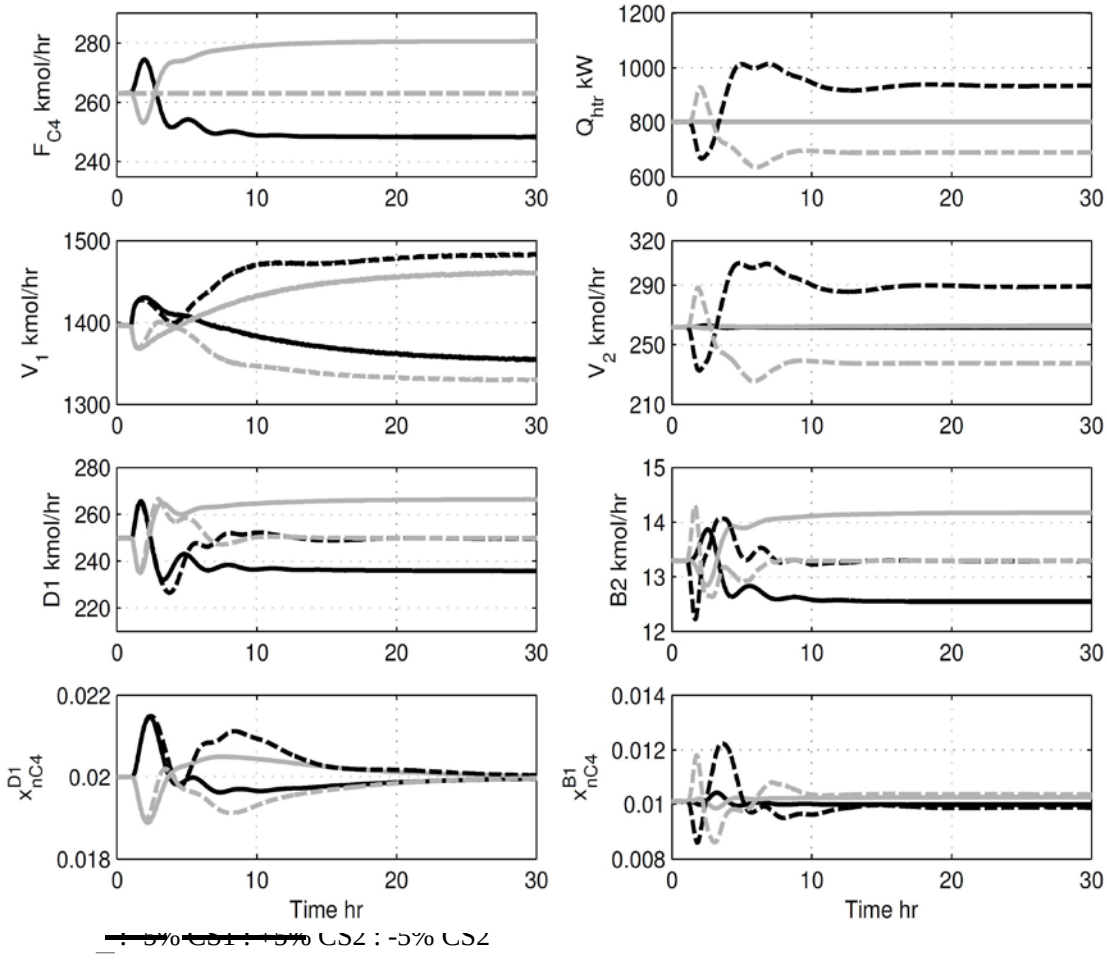

Figure 17.6 plots the Mode I dynamic response for a ±20 kmol/h change in F_{C4}. In CS1, the Q_{htr} setpoint must be increased (decreased) by 169 kW (~21% of base-case Q_{htr}) to bring about a 20 kmol/h (~7.6% of base-case F_{C4}) increase in F_{C4}. Similarly, Q_{htr} must be decreased by 138 kW (~17.2%) for achieving the decrease in F_{C4}. For the throughput change disturbance, the product impurity is well controlled in the transient period in both CS1 and CS2. The transient deviations in CS1 are slightly lower than in CS2 due to more severe transients in the recycle loop in the latter. In CS1 on the other hand, the recycle loop transients are less severe (smooth response). In addition to tight product impurity control, both the structures achieve tight regulation of the $n\text{-}C_4$ leakage in the purge column bottoms via the action of the T^{S}_{pur} controller. The transient variability in x^{B2}_{nC4} is significantly higher in CS1 as a large change in Q_{htr} (TPM) causes a large change in D_2 which severely disturbs the purge column material balance.

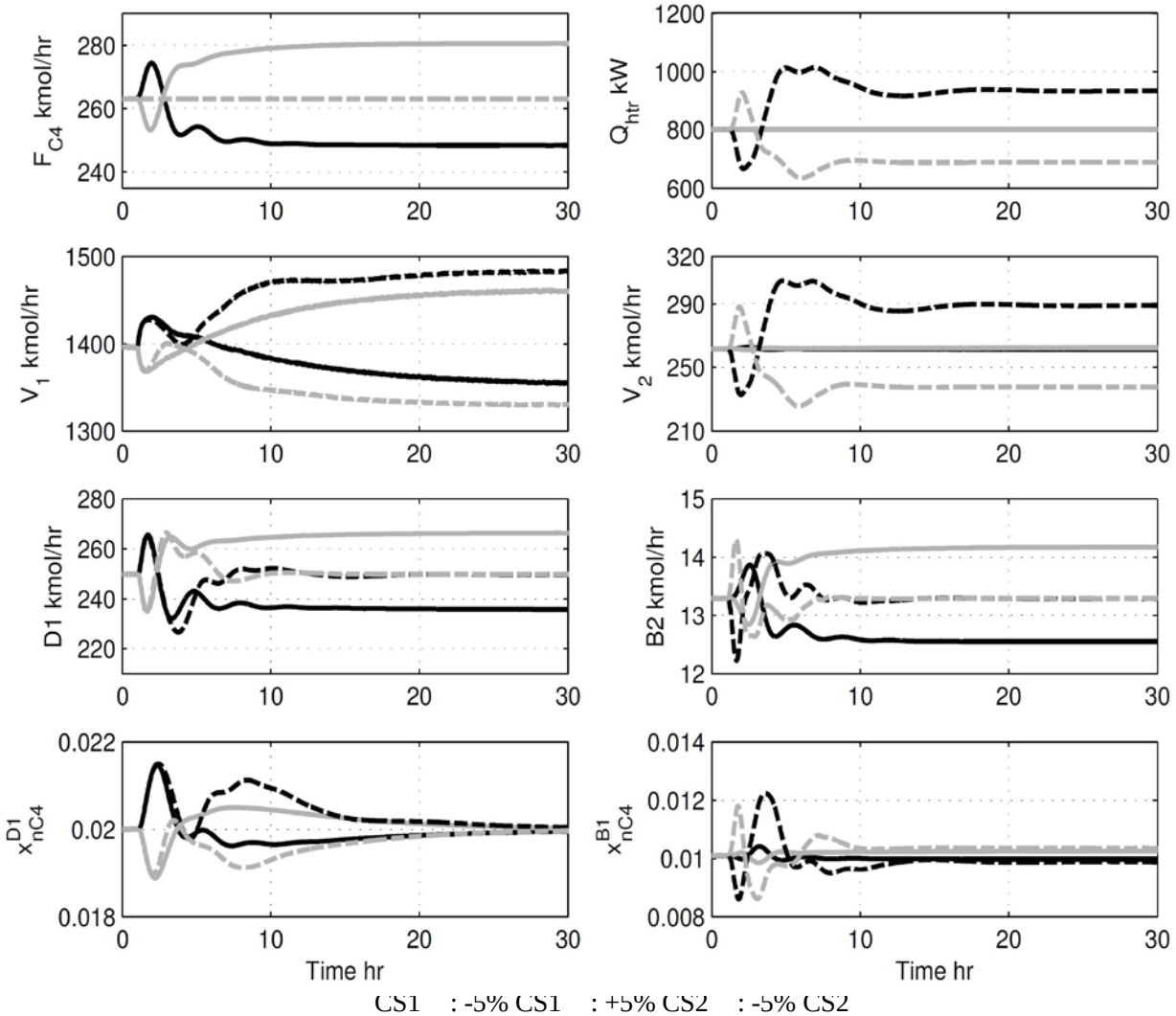

Figure 17.7 plots the Mode II dynamic response to a ±5% feed composition step change. All override controllers in CS2 are active so that structurally, CS1 and CS2 are very similar. The only significant difference is that the setpoint of the T_{rxr} and T^{s}_{pur} override controllers in CS2 is slightly lower than the corresponding nominal setpoint values. In CS1, on the other hand, the setpoint values are held at their nominal values. As seen from the dynamic responses, the plantwide transient response is smooth in both the structures. Also, tight control of product impurity and the *n*-C_4 leakage down the purge column bottoms is achieved. In CS2 however, the production of *i*-C_4 at the initial and final steady state is slightly lower than in CS1 due to the slightly lower T_{rxr} setpoint which causes a slight reduction in single pass reactor conversion as well as higher *n*-C_4 leakage in the purge column bottoms due to the lower T^{s}_{pur} setpoint.

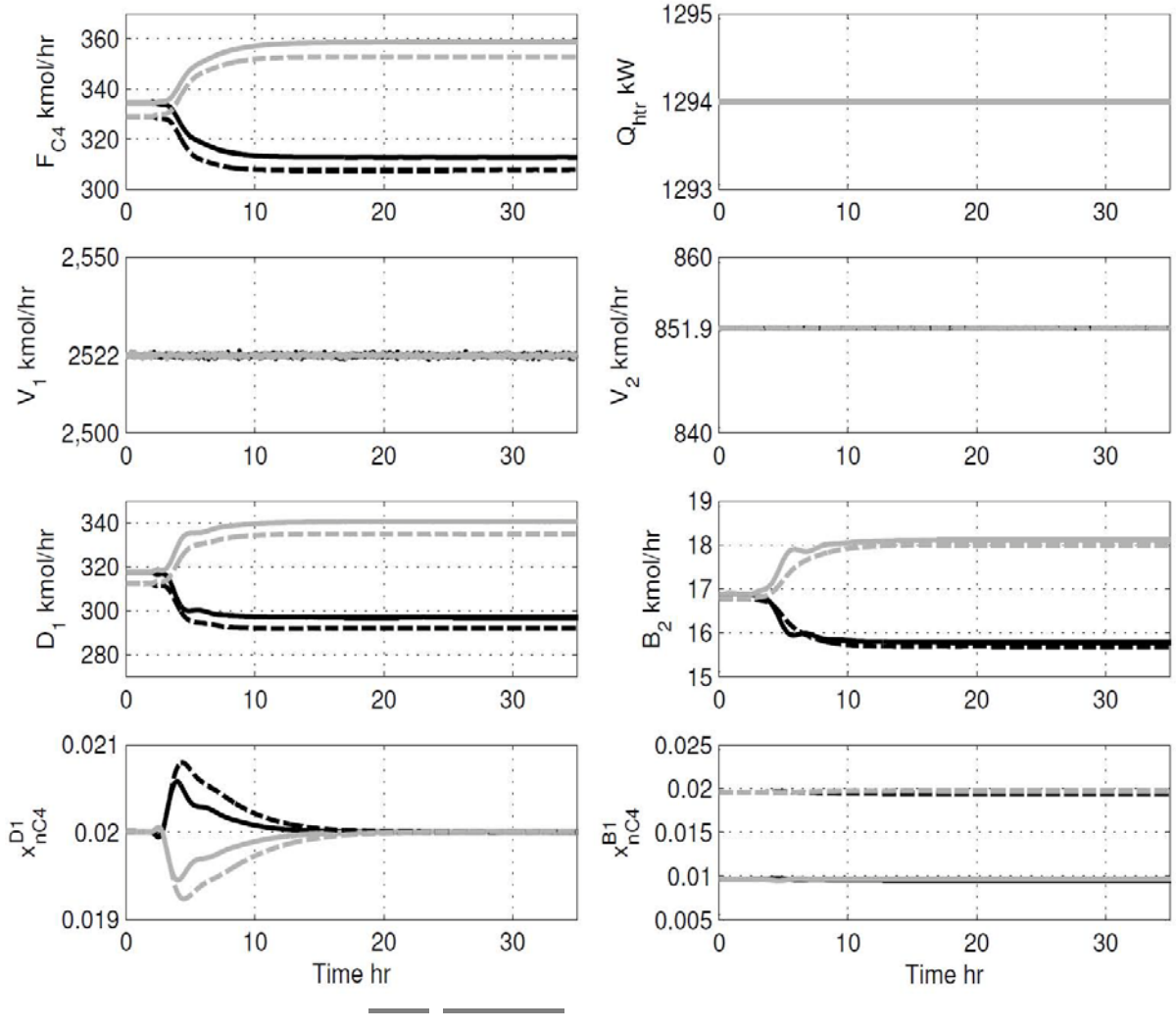

The synthesized control structures are also tested for a large throughput transition from the design throughput (F_{C4} = 263.1 kmol/h) to the maximum achievable throughput and back. The transient response is shown in Figure 17.8. In CS1, to increase throughput, the split range scheme switches the TPM from Q_{htr} to ΔT^{SP}_{DIB} and then to V_2/B_1. The switching order gets reversed for decreasing the throughput. The transient response shows that tight product impurity

control is achieved across the entire throughput range. The loss of precious *n*-C_4 down B_2 is also regulated at a small value. Most importantly, the plantwide transients are smooth and not too severe.

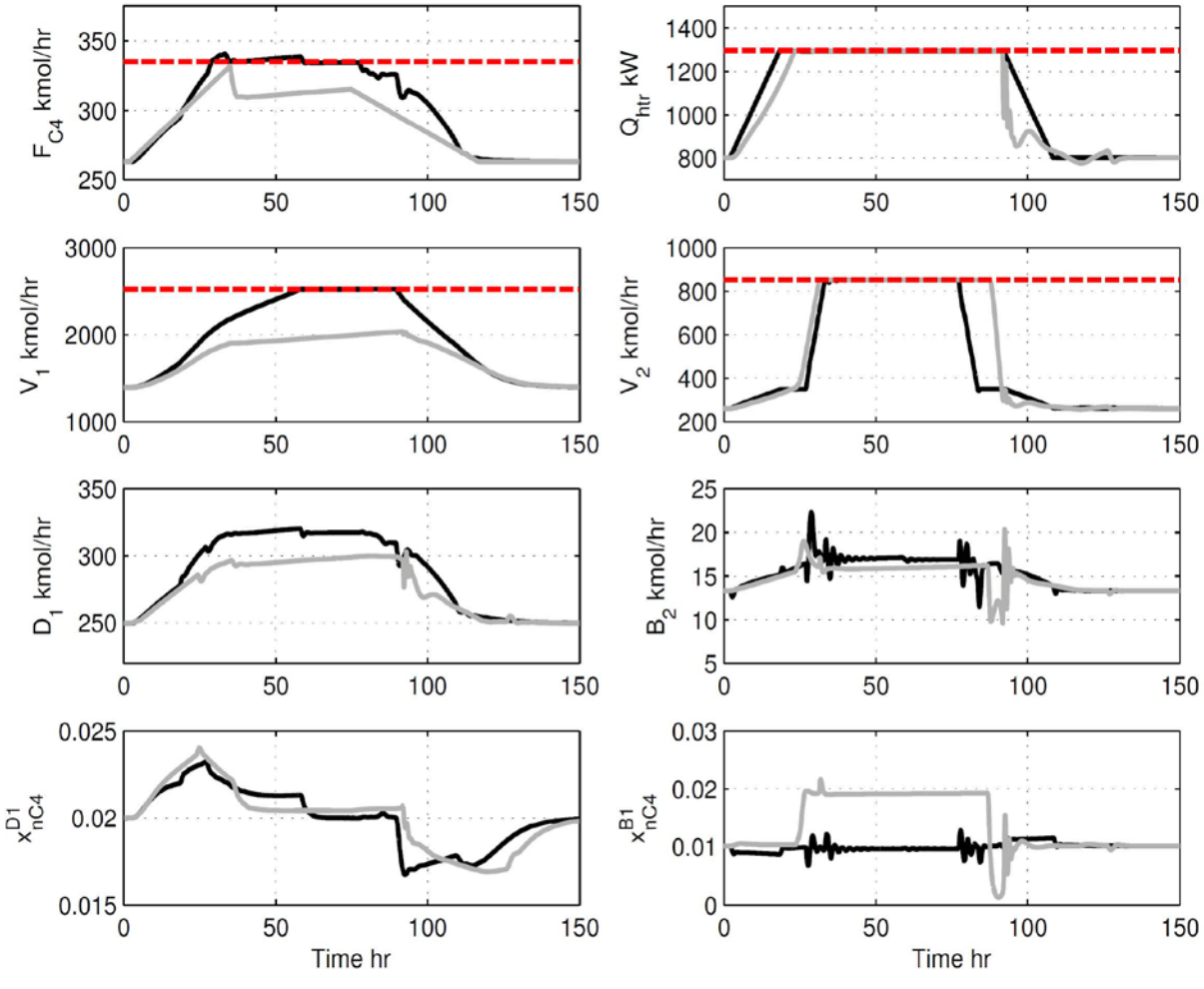

steady throughput MAX MAX MAX MAX

In CS2, F_{C4}^{SP} is ramped up causing Q_{htr} to increase and as it crosses the Q_{htr} override controller setpoint (chosen setpoint is 95% of Q_{htr}^{MAX}), the override output increases above the ΔT_{DIB} controller output passing V_1^{SP} manipulation to the Q_{htr} override, which slowly keeps on increasing V_1 to $V_1^{SP\,MAX\,MAX}$. As and when Q_{htr} is reached, T_{rxr} decreases and the override $T_{rxr\,SP\,MAX}$ controller takes over D_2 manipulation. Meanwhile, V_2 increases rapidly and hits V_2 as more *n*-C_4 is being fed in than being consumed in the reactor. This causes T_s *pur* to decrease and the override scheme for altering the material balance structure gets activated to cut the F_{C4} feed. Since the Q_{htr} override is a long loop, the increase in V_1 is slow and even after 75 hrs, the V_1^{MAX} constraint is not approached and the product rate, D_1, is about 299 kmol/h (~20 kmol/h < maximum steady D_1). Even as D_1 reaches its maximum steady value, it takes a very long time. After 75 hrs, F_{C4}^{SP} is ramped down to its base value (263.1 kmol/h) and a smooth transition

occurs. From the CS2 response in Figure 17.8, notice that in the small period where V_2^{MAX} goes active and T_{pur}^{S} override starts manipulating B_1, large transient loss of precious *n*-C_4 down the purge column bottoms occurs. Also, the steady *n*-C_4 loss is higher due to the lower than nominal setpoint of the T_{pur}^{S} override.

Another pertinent comparison is the transients caused due to overrides taking over / giving up control during routine disturbances. We consider a worst-case step disturbance in the fresh feed composition, where the *n*-C_4 composition increases by 5% with initial steady operation at F_{C4} = 293.1 kmol/h, where none of the constraints are active. The transient response of CS1 and CS2 to this disturbance is shown in Figure 17.9. CS1 effectively rejects the disturbance with tight product purity control and regulation of *n*-C_4 in the purge column bottoms with the plant settling down at the new steady state in about 30 hrs. In CS2, on *n*-C_4 composition increasing by 5%, a large transient increase occurs in Q_{htr} due to the snowball effect[12], which triggers the Q_{htr} override. V_1 is then slowly driven towards V_1^{MAX} while the additional *n*-C_4 causes V_2 to increase. The slow increase in V_2 causes the *i*-C_5 circulating in the plant and hence D_2 to decrease. For the lower D_2 (reactor feed), T_{rxr} control eventually passes back to Q_{htr} and the plant settles at the new steady state in about 75 hrs, which is more than twice the time for CS1. If the Q_{htr} override controller is made aggressive by increasing the proportional gain by a factor of 2, oscillations due to the T_{rxr} override successively going active and inactive are observed (see Figure 17.9). The dynamic performance thus degrades significantly at high throughputs where the overrides get activated. It is then not surprising at all that operators tend to switch the overrides off and make the necessary adjustments manually.

17.4.3. Quantitative Economic Performance Comparison

A quantitative economic comparison of the two control structures is performed for maximum throughput (Mode II) operation. We consider a +5% feed *n*-C_4 composition step change as the worst case disturbance. Table 17.4 compares the maximum achieved steady throughput (F_{C4}) along with the corresponding *n*-C_4 component flow (loss) in the purge column bottoms, the *i*-C_4 product rate and the operating yearly profit for CS1 and CS2. Expectedly, no back-off and throughput loss is observed for CS1, which has been designed for process operation with all the hard active constraints at their maximum limits. In contrast, in CS2, due to the need for the T_{rxr} and T_{pur}^{S} override setpoints to be lower than nominal, an yearly profit loss of $\$0.45 \times 10^{6}$ (~2%) occurs compared to CS1. The override controller setpoint offsets have been chosen to be as small as possible at 1 °C for T_{rxr} and 5 °C for T_{pur}^{S} to ensure that the overrides do not get triggered during routine transients. CS2, which was obtained without any consideration of the constraints that go active at higher throughputs, thus is economically and dynamically inferior to CS1 regardless of the approach used to handle constraints (back-off or overrides). Overall, these results demonstrate that the full active constraint set plays a key role in economic plantwide control system design.

17.5. Conclusions

In conclusion, this case study on plantwide control of the C_4 isomerization process demonstrates that a simple decentralized plantwide control system for achieving near optimal and smooth process operation over a wide throughput range can be synthesized. The active constraints at maximum throughput form the key to devising the control system. These

constraints dictate the pairings for tight control of these active constraints and the consequent pairings for inventory regulation as well as the throughput manipulation strategy. Quantitative results show that a conventional control structure with the TPM at the process feed with overrides for handling constraints is economically inferior with a steady profit loss of ~2% at maximum throughput due to the offset needed in the override controller setpoints. The conventional scheme is also found to be dynamically inferior. The case study demonstrates the crucial role of the active constraints in economic plantwide control structure synthesis.

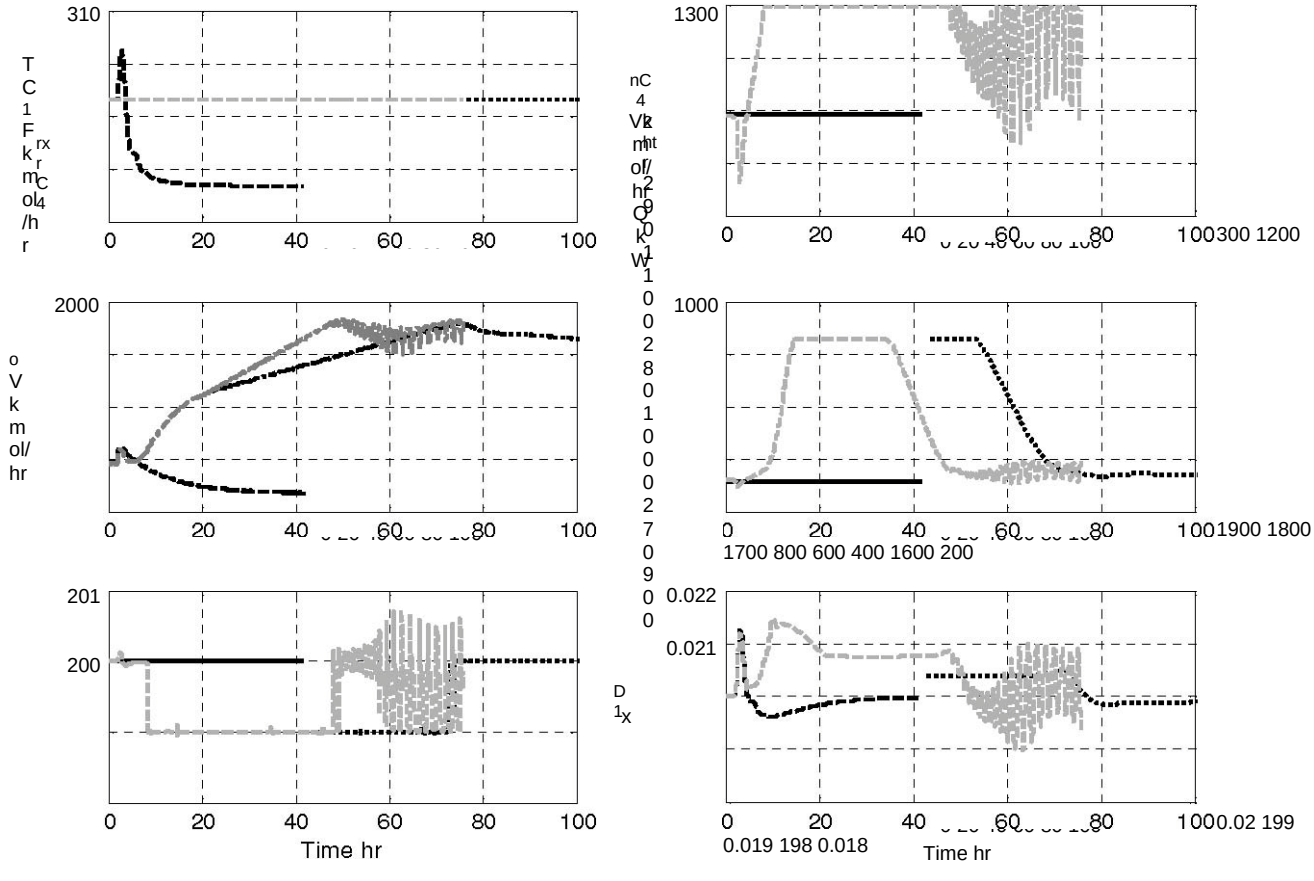

Figure 17.9. Transient response for +5% feed n-C_4 composition change at F_{C4} = 293.1kmol/hr : CS1 : CS2 aggressive Q_{htr} override : CS2 loose Q_{htr} override

Table 17.4. Mode II throughput loss comparison for +5 mol% feed composition step change

i	Reaction	k_i	*CS1 CS2* $E_{a\,i}$ *(kJ/kmol)*	Concentration terms $f_i(C_j)$
1	$C_6H_6 + C_3H_6 - C_9H_{12}$	2.8 x 10^7	104174	$C_{C3}C_{C6}$
2	$C_9H_{12} + C_3H_6 - C_{12}H_{18}$	2.32 x 109	146742	$C_{C3}C_{C9}$
Objective		Maximize(*J*) *J*: hourly operating profit *		
		0 ≤ Material Flows ≤ 2 (base case) 0 ≤ V_1, V_2, V_3 ≤ 1.5 (base		

Bibliography

1. Al-Arfaj MA, Luyben WL. Plantwide control for TAME production using reactive distillation. *AIChE J.* 2004;50(7):1462-1473.

2. Araujo A, Skogestad S. Control structure design for the ammonia synthesis process. *Comp Chem Eng.* 2008;32(12):2920-2932.

3. Aske EMB, Strand S, Skogestad S. Coordinator MPC for maximizing plant throughput. *Comp Chem Eng.* 2008;32:195-204.

4. Aske EMB, Skogestad S. Consistent inventory control. *Ind Eng Chem Res.* 2009;48(44): 10892-10902.

5. Douglas JM. *Conceptual Design of Chemical Processes*. New York: McGraw Hill, 1988.

6. Gera V, Kaistha N, Panahi M, Skogestad S. Plantwide control of a cumene manufacture process. *Computer Aided Chemical Engineering*, 2011, *29* (8), 522-526.

7. Jagtap R, Kaistha N, Skogestad S. Plantwide control for economic optimum operation of a recycle process with side reaction. *Ind Eng Chem Res.* 2011;50(14):8571-8584.

8. Jagtap R, Kaistha N. Economic plantwide control of the ethyl benzene process. *AIChE J.* 2012; submitted.

9. Jagtap R, Kaistha N. Economic plantwide control of the C_4 isomerization process. *Ind Eng Chem Res.* 2012; submitted.

10. Jagtap R, Kaistha N. Throughput manipulator location selection for economic plantwide control. In Rangaiah GP, Kariwala VA. *Advances in Plantwide Control*. Upper Saddle River NJ: John Wiley and Sons, 2012 in press.

11. Kanodia R, Kaistha N. Plantwide control for throughput maximization: A case study. *Ind Eng Chem Res.* 2010;49(1):210-221.

12. Luyben M.L, Luyben W.L. Design and control of a complex process involving two reaction steps, three distillation columns, and two recycle streams. *Ind. Eng. Chem. Res.* 1995, *34* (11), 3885-3898.

13. Luyben M.L, Tyreus B.D, Luyben W.L. Analysis of control structures for reaction/separation/recycle processes with second order reactions. *Ind. Eng. Chem. Res.* 1996, *35* (3), 758-771.

14. Luyben ML, Tyreus BD, Luyben WL. Plantwide control design procedure. *AIChE J.* 1997;43(12):3161-3174.

15. Luyben WL. Snowball effects in reactor/separator processes with recycle. *Ind Eng Chem Res.* 1994;33(2):299-305.

16. Luyben WL, Tyreus BD, Luyben ML. *Plantwide Process Control*. New York: McGraw Hill, 1999.

17. Luyben WL, Tyreus BD, Luyben ML. Isomerization process, *Plantwide Process Control*, McGraw Hill: New York, 1999, 273-293.

18. Luyben WL. Plantwide control of an isopropyl alcohol dehydration process. *AIChE J.* 2006;52(6):2290-2296.

19. Luyben WL. Design and control of the cumene process. *Ind. Eng. Chem. Res.* 2010, *49* (2), 719.

20. Price RM, Lyman PR, Georgakis C. Throughput manipulation in plantwide control structures. *Ind Eng Chem Res.* 1994;33(5):1197-1207.

21. Shinskey FG. *Process Control Systems: Application, Design and Tuning*. New York: McGraw Hill, 1996.

22. Singh S, Lal S, Kaistha N. Case study on tubular reactor hot-spot temperature control for throughput maximization. *Ind Eng Chem Res.* 2008;47(19):7257-7263.

23. Skogestad S. Plantwide control: The search for the self-optimizing control structure. *J Proc Cont.* 2000, 10(5), 487-507.

24. Skogestad S. Control structure design for complete chemical plants. *Comp Chem Eng.* 2004;28(1-2):219-234.

25. Skogestad S. Do's and dont's of distillation control. *Chem Eng Res Des (Trans I ChemE, Part A).* 2007;85(A1):13-23.

26. Tyreus BD, Luyben WL. Dynamics and control of recycle systems 4. Ternary systems with one or two recycle stream. *Ind. Eng. Chem. Res.* 1993, *32* (6), 1154-1162.

27. Zhang C, Vasudevan S, Rangaiah GP. Plantwide control system design and performance evaluation for ammonia synthesis process. *Ind Eng Chem Res.* 2010;49(24):12538-12547.